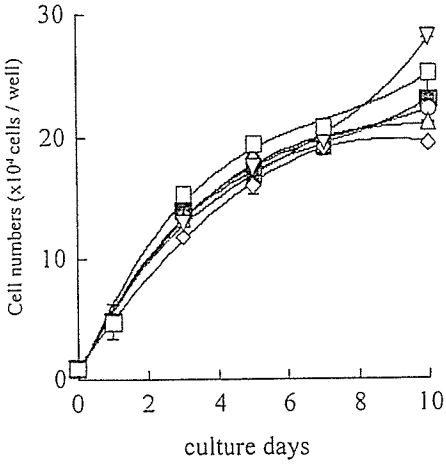

Fig.2 Effect of 0.5mg/ml hyaluronan on the proliferation of rOB cells

■ none ○ Hya0.2 △ Hya2 ◇ Hya30 ▽ Hya90 □ Hya120

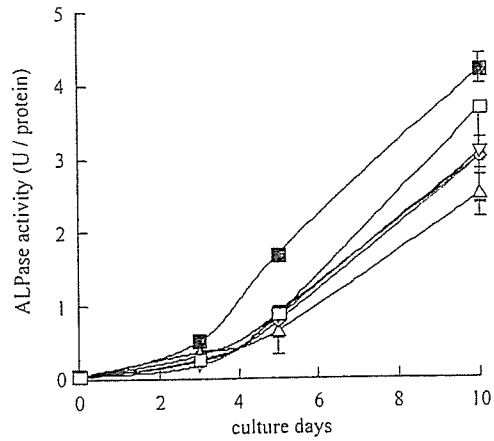

Fig.4 Effect of 0.5mg/ml hyaluronan on the ALPase activity of rOB cells

■ none ○ Hya0.2 △ Hya2 ◇ Hya30 ▽ Hya90 □ Hya120

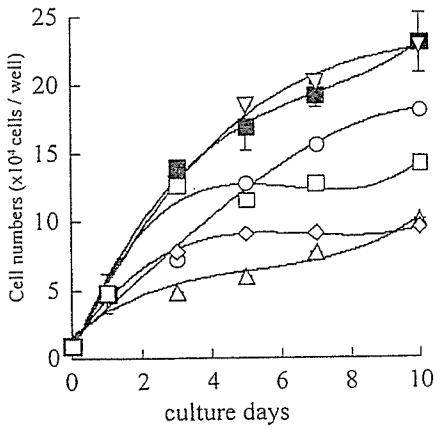

Fig.3 Effect of 0.5mg/ml sulfated polysaccharides on the proliferation of rOB cells

■ none ○ 1.2SHya △ 2.1SHya ◇ 3.4SHya ▽ Chs-C □ Hep

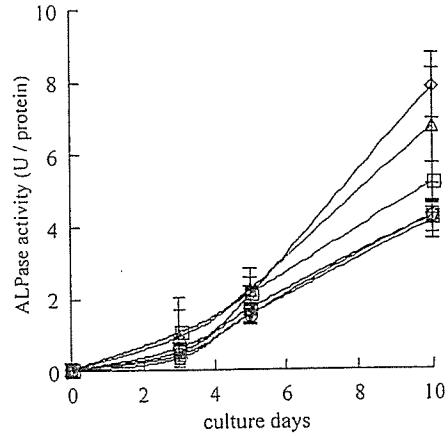

Fig.5 Effect of 0.5mg/ml sulfated polysaccharides on the ALPase activity of rOB cells

■ none ○ 1.2SHya △ 2.1SHya ◇ 3.4SHya ▽ Chs-C □ Hep

た.

Fig. 3 に，硫酸化度の異なる SHya を添加した rOB cells の増殖曲線を示した． Hya を添加した場合と異なり，SHya を添加した rOB cells は，培養 3 日目から非添加系に比べて増殖が抑制された． さらに，SHya の硫酸基の導入率が高くなるほど，rOB cells の増殖は抑制された． これに対し，同じ硫酸基を有する多糖類であっても Chs-C ではほとんど影響は見られず，Hep でも抑制効果は小さかった．

Fig. 4 に，Hya を添加した rOB cells のアルカリフォスファターゼ(ALPase)活性の経時変化を示した． Hya は分子量に関係無く，骨芽細胞の初期分化マーカーである ALPase の活性は非添加系に比べて低い値を示した．Fig. 5 に、硫酸化度の異なる SHya を添加した rOB cells の ALPase 活性を示した． Hya とは異なり，SHya を添加した rOB cells の ALPase 活性は非添加系に比べて上昇が認められた． 特に、高硫酸化度になるほど，ALPase 活性の

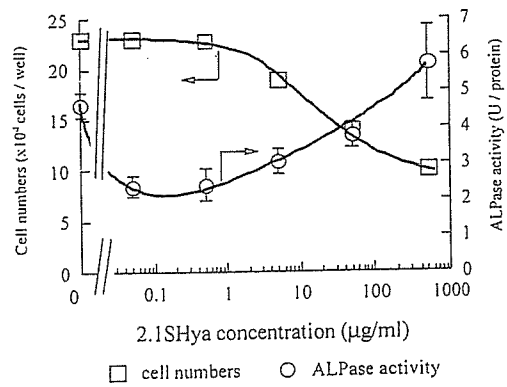

Fig.6 Dose-dependence of 2.1SHya on the proliferation and ALPase activity of rOB cells after 10days

上昇率は高かった．そこで，rOB cells の増殖と ALPase 活性に対する 2.1SHya の添加濃度の影響を検討した (Fig.6)．高濃度の SHya は rOB cells の増殖を抑制し，ALPase 活性を促進させたのに対し，低濃度の SHya は増殖を促進し，ALPase 活性を抑制させることが認められた．

4. 考察

本実験で我々は，分子量の異なる Hya を骨芽細胞に添加し，骨芽細胞の増殖と ALPase 活性について検討を行った．分子量 2000 から 120 万の Hya を rOB cells に添加したところ 非添加系とほとんど変わりなく増殖し，Hya 添加やその分子量の違いによる影響は見られなかった (Fig.2)．しかし，ALPase の活性は分子量に関係なく非添加系に比べてすべて低いため (Fig.4)，Hya は rOB cells の分化を抑制することが示唆された．Hep, HS は細胞外あるいは細胞表面に広く存在し，多くの種類のタンパク質と特異的な相互作用を示すことが知られている[18]．特に，ヘパラン硫酸プロテオグリカン (HSPG) は，細胞と ECM の相互作用や細胞同士の相互作用を介して，接着，凝集，シグナル伝達などに関与している．このように，多岐にわたる HSPG の機能の中で，増殖因子との相互作用については多くの報告があり，注目されている[1-3]．FGF, transforming growth factor-β(TGF-β), bone morphogenetic protein(BMP)などの細胞増殖因子は，Hep や HS などの硫酸化多糖と相互作用し，細胞の増殖を制御することが報告されている[1,4]．Hep, HS, Chs の分子量は，Hya に比べて非常に小さい．そこで本研究では，高分子量である SHya の骨再生用材料への応用を目的として，SHya 単独での rOB cells に対する影響を検討した．SHya の硫酸化度が高くなるにつれ，細胞の増殖は抑制され，Hep もある程度の抑制効果を示した(Fig.3)．ALPase 活性に対しては，硫酸化度が高くなるにつれて活性が上昇した(Fig.5)．これより，硫酸化多糖は細胞の増殖を抑制し，分化を促進させることが示された．次に，影響が最も大きく現れた 2.1SHya を用いて，濃度依存性について検討を行った．Fig.6 より，2.1SHya は低濃度では細胞の増殖を促進し，高濃度になるにつれ増殖を抑制した．これに対して ALPase 活性は低濃度では活性が低く，高濃度になるにつれ上昇した．これより，2.1SHya は濃度を変化させることで，rOB cells の機能を制御することが可能であることが示された．Hep, HS と増殖因子との協同的な作用の細胞の増殖に対する影響も，濃度によって大きく異なることが報告されている．Blanquaert らは，Hep 及び硫酸化多糖の RGTA(Heparin-like polymers derived from dextran)と増殖因子との協同作用による，マウス頭蓋冠由来骨芽細胞 MC3T3-E1 への影響を報告している[1]．RGTA は増殖因子と共に用いることで，増殖に対しては抑制的に働き，ALPase の活性が上昇することを明らかにした．この作用は RGTA のみでも影響が現れるが，増殖因子が存在することにより，さらに顕著に影響が現れた．今回，我々は SHya 単独の影響を検討したが，彼らの結果と一致する結果が得られた．以上の結果から，Hya に硫酸基を導入することにより，SHya は骨芽細胞の増殖や分化機能を制御することが可能であると示された．

5. 結論

rOB cells に Hya を添加すると，rOB cells の増殖は促進され，分化は抑制された．しかし，SHya を添加すると，rOB cells の増殖は抑制され，分化の促進が示された．SHya の効果は SHya の硫酸化度，濃度に大きく依存した．従って，SHya は骨芽細胞の機能を制御することが明かとなった．骨形成促進作用を持っている BMP, FGF2, TGF-β などの増殖因子を臨床応用に用いる場合，これらの増殖因子に適した担体の開発が必要である．SHya は分子量が高く，粘性があるため，増殖因子を保持する能力は Hep、HS などの他の硫酸化多糖に比べて高いことが考えられる．今後，SHya と増殖因子との相互作用について検討を行うことにより，SHya の分化促進作用の機序を明らかにできると同時に，SHya の骨再生用材料への応用が期待される．

6. 謝辞

本研究の一部は，21 世紀 COE プログラム，科学研究費補助金基盤研究(B)(14350495)，創薬等ヒューマンサイエンス総合研究事業，厚生労働科学研究費補助金（萌芽的先端医療技術推進研究，医薬品・医療機器等レギュラトリーサイエンス総合研究事業）の助成金により行われた．

文献

1. F. Blanuaert, D. Barritault and J. P. Caruelle, *J. Biomed. Mater. Res.*, **44**, 63 (1999)
2. E. Ruoslahti and D. Yamaguchi, *Cell*, **64**, 867 (1991)
3. O. Saksela, D. Moscatelli, A. Sommer and D.B. Rifkin, *J. Cel.l Biol.*, **107**, 743 (1988)
4. D. J. Baylink, R. D. Finkelman and S. E. Mohan, *J. Bone Miner. Res.*, **8**, S565 (1993)
5. W. T. Bourque, M. Gross and B. K. Hall, *Int. J. Dev. Biol.*, **37**, 573 (1993)
6. M. E. Joyce, S. Jingushi , S. P. Scully and M. E. Bolander, Preg. *Clin. Biol. Res.*, **365**, 391 (1991)
7. H. Ueda , L. Hong , M. Yamamoto, K. Shigeno, M. Inoue, T. Toba, M. Yoshitani, T. Nakamura, Y. Tabata and Y. Shimizu, *Biomaterials*, **23**, 1003

(2002)
8. C. H. Tang, R. S. Yang, H. C. Liou and W. M. Fu, *J. Biomed. Mater. Res.*, **63**, 577 (2002)
9. P. H. Weigel, V. C. Hascall and M. Tammi, *J. Biol. Chem.*, **272**, 13997 (1997)
10. W. Zhang, C. E. Watson, C. Liu, K. J. Williams and V. P. Werth, *Biochem. .J.*, **349**, 91 (2000)
11. L. S. Liu, C. K. Ng, A. Y. Thompson, J. W. Poser and R. C. Spiro, *J. Biomed. Mater. Res.*, **62**, 128 (2002)
12. L. Sherma, J. Sleeman, P. Herrlich and H. Ponta, *Curr. Opin. Cell. Biol.*, **6**,726 (1994)
13. P. W. Kincade,Z. Zheng, S. Katoh and L. Hanson, *Curr. Opin. Cell. Biol.*, **9**, 635 (1997)
14. J. Entwistle, C. L. Hall and E. A. Turley, *J. Cell Biochem.*, **61**, 569 (1996)
15. A. Pilloni and G. W. Bernard, *Cell Tissue. Res.*, **294**, 323 (1998)
16. M. Nagahata, T. Tsuchiya, T. Ishiguro, N. Matsuda, Y. Nakatsuchi, A. Teramoto, A. Hachimori and K. Abe, *Biochem. Biophys. Res. Commun..*, **315**, 603-611 (2004)
17. T. Hamano, D. Chiba, K. Nakatsuka, M. Nagahata, A. Teramoto, Y. Kondo, A. Hachimori and K. Abe, *Polym. Adv. Technol.*, **13**, 46 (2002)
18. E. Ruoslahti, *Ann. Rev. Cell. Biol.*, **4**, 229 (1988)

Novel mechanism of tumorigenesis: Increased transforming growth factor-β1 suppresses the expression of connexin 43 in BALB/cJ mice after implantation of poly-L-lactic acid

Saifuddin Ahmed, Toshie Tsuchiya
Division of Medical Devices, National Institute of Health Sciences, 1-18-1, Kamiyoga, Setagaya ku, Tokyo 158-8501, Japan

Received 15 December 2003; revised 24 March 2004; accepted 6 April 2004
Published online 4 June 2004 in Wiley InterScience (www.interscience.wiley.com). DOI: 10.1002/jbm.a.30090

Abstract: Poly-L-lactic acid (PLLA) is a widely used promising material for surgical implants such as tissue-engineered scaffolds. In this study, we aimed to determine the *in vivo* effect of PLLA plates on the cellular function of subcutaneous tissue in the two mouse strains, BALB/cJ and SJL/J, higher and lower tumorigenic strains, respectively. Gap-junctional intercellular communication (GJIC) and the expression of connexin 43 (Cx43) protein were significantly suppressed, whereas the secretion of transforming growth factor-β1 (TGF-β1) level was significantly increased in PLLA-implanted BALB/cJ mice compared with BALB/cJ controls. However, no significant difference in TGF-β1 secretion was observed between the SJL/J-implanted and SJL/J control mice. We found for the first time that a significant difference was observed between the two strains; thus, the PLLA increased the secretion of TGF-β1 and suppressed the mRNA expression of Cx43 at the earlier stage after implantation into the higher-tumorigenic strain, BALB/cJ mice. This novel mechanism might have a vital role in the inhibition of GJIC and promote the tumorigenesis in BALB/cJ mice. © 2004 Wiley Periodicals, Inc. J Biomed Mater Res 70A: 335–340, 2004

Key words: poly-L-lactic acid; gap-junctional intercellular communication (GJIC); connexin 43; transforming growth factor (TGF)-β; tumorigenesis

INTRODUCTION

The implantation of a biomaterial always induces a host inflammatory response. The extent and resolution of these responses have a vital role in determining the long-term success of implanted medical devices.[1–3] Poly-L-lactic acid (PLLA) is a widely used material for surgical implants and clinically as a bioabsorbable suture material.[4,5] Polyurethanes (PUs) have also been used for implant applications because of their useful elastomeric properties and high tensile strength, lubricity, and good abrasion resistance. Some adverse effects of the biomaterials, such as PLLA and PUs, have been reported in animal experiments. Long-term implants of PLLA produced tumorigenicity in rats.[6] Different kinds of PUs induced various tumor incidences in rats.[7] All tumors have been generally viewed as the outcome of disruption of the homeostatic regulation of the cellular ability to respond to extracellular signals, which trigger intracellular signal transduction abnormalities.[8] During the evolutionary transition from the single-cell organism to the multicellular organism, many genes appeared to accompany these cellular functions. One of these genes was the gene coding for a membrane-associated protein channel (the gap junction).[9] Gap-junctional intercellular communications (GJIC) are transmembrane channels that allow the cell–cell transfer of small molecules and are composed of protein subunits known as connexin; at least 19 connexins exist and they are expressed in a cell- and development-specific manner.[10,11] GJIC also has an important role in the maintenance of cell homeostasis and in the control of cell growth.[12] So, the loss of GJIC has been considered to cause abnormal development and tumor formation.[13–15] Several tumor promoters have been shown to restrict GJIC by phosphorylation of connexin proteins, such as connexin 43 (Cx43), which is an essential

Correspondence to: T. Tsuchiya; e-mail: tsuchiya@nihs.go.jp
Contract grant sponsor: Health and Labour Sciences Research Grants
Contract grant sponsor: Research on Advanced Medical Technology, Ministry of Health, Labour and Welfare
Contract grant sponsor: Japan Health Sciences Foundation

protein to form the gap-junction channel.[16,17] We have hypothesized that the different tumorigenic potentials of PLLA and PUs are caused mainly by the different tumor-promoting activities of these biomaterials. Therefore, we investigated the effects of PLLA on the subcutaneous tissue between the two strains of female mice, BALB/cJ and SJL/J.

MATERIALS AND METHODS

Animals

Five-week-old female BALB/cJ and SJL/J mice were purchased from Charles River (Japan) and maintained in the animal center according to the animal welfare National Institute of Health Sciences guidance. All mice were fed with standard pellet diets and water *ad libitum*, before and after the implantation.

Implantation of PLLA

PLLA was obtained from Shimadzu Co. Ltd. as uniform plates. Implants (size: 20 × 10 × 1 mm, weight-average molecular weight 200,000) were sterilized using ethylene oxide gas before use. Sodium pentobarbital (4 mg/kg) was intraperitoneally administered to the mice. The dorsal skin was shaved and scrubbed with 70% alcohol. Using an aseptic technique, an incision of approximately 2 cm was made; away from the incision, a subcutaneous pocket was formed by blunt dissection, and one piece of PLLA was placed in the pocket. The incision was closed with silk threads. In both strains, controls were obtained by sham operation and subsequent subcutaneous pocket formation. After surgery, the mice were housed in individual cages. After 30 days, mice from the implanted group were sacrificed, implanted materials were excised out, and subcutaneous tissues from the adjacent sites were collected for culture. At the same time, subcutaneous tissues were removed from the sites in the sham-operated controls that correlated with the implant sites.

Cell culture of subcutaneous tissues

The subcutaneous tissues were maintained in minimum essential medium supplemented with 10% fetal bovine serum in a 5% CO_2 atmosphere at 37°C.

Scrape-loading and dye transfer (SLDT) assay

SLDT technique was performed by the method of El-Fouly et al.[18] Confluent monolayer cells in 35-mm culture dishes were used. After rinsing with Ca^{2+} Mg^{2+} phosphate-buffered saline [PBS (+)], cell dishes were loaded with 0.1% Lucifer Yellow (Molecular Probes, Eugene, OR) in PBS (+) solution and were scraped immediately with a sharp blade. After incubation for 5 min at 37°C, cells were washed three times with PBS (+) and the extent of dye transfer was monitored using a fluorescence microscope, equipped with a type UFX-DXII CCD camera and super high-pressure mercury lamp power supply (Nikon, Tokyo, Japan).

Western blot analysis

When cells grew confluently in 60-mm tissue culture dishes, all cells were lysed directly in 100 μL of 2% sodium dodecyl sulfate (SDS) gel loading buffer (50 m*M* Tris-HCl, pH 6.8, 100 m*M* 2-mercaptoethanol, 2% SDS, 0.1% bromophenol blue, 10% glycerol). The protein concentration of the cleared lysate was measured using the microplate BCA (bicinchoninic acid) protein assay (Pierce, Rockford, IL). Equivalent protein samples were analyzed by 7.5% SDS–polyacrylamide gel electrophoresis. The proteins were transferred to Hybond-ECL nitrocellulose membranes (Amersham Pharmacia Biotech UK Ltd., Buckinghamshire, UK). Cx43 protein was detected by anti-Cx43 polyclonal antibodies (ZYMED Laboratories, Inc., San Francisco, CA). The membrane was soaked with Block Ace (Yukijirusi Nyugyo, Sappro, Japan), reacted with the anti-Cx43 polyclonal antibodies for 1 h, and after washes with PBS containing 0.1% Tween20, reacted with the secondary anti-rabbit immunoglobulin G antibody conjugated with horseradish peroxidase for 1 h. After several washes with PBS–Tween20, the membrane was detected with the ECL detection system (Amersham Pharmacia Biotech UK Ltd.).

Reverse transcriptase polymerase chain reaction (RT-PCR)

Cx43 mRNA expression was verified by RT-PCR. Total cellular RNA was isolated from cultured cells in Trizol reagent (Life Technologies, Inc., Frederick, MD) following the manufacturer's instructions. The concentration of total RNA was determined using a UV spectrophotometer (Gene Quant; Pharmacia Biotech, Piscataway, NJ). cDNA was synthesized from 1 μg of total RNA by RT using the First-Strand cDNA synthesis kit (Amersham Pharmacia Biotech, Uppsala, Sweden). Amplification was performed in a volume of 25 μL containing 1 μL of cDNA, 10 pmol of each primer, 0.625 unit of *Taq* polymerase (Promega, Madison, WI) and 0.2 m*M* of each deoxynucleotide triphosphate. The sequence of the primer pairs were as follows: forward 5′-ACAGTCTGCCTTTCGCTGTAAC-3′ and reverse 5′-GTAAGGATCGCTTCTTCCCTTC-3′. The PCR cycle was as follows: initial denaturation at 94°C for 5 min, followed by 25 cycles of 94°C for 1 min, 60°C for 1 min, and 72°C for 1 min, with final extension at 72°C for 7 min. The amplified product was separated on 1.5% agarose gel and visualized with SYBR Green I (BioWhittaker Molecular Applications, Rockland, ME). For relative quantitation, the signal intensity of each lane was standardized to that of a housekeeping gene,

GAPDH. To amplify this gene, the following primer pairs were used: forward 5′-CCCATCACCATCTTCCAGGAGC-GAGA-3′ and reverse 5′-TGGCCAAGGTCATCCATGA-CAACTTTGG-3′.

Enzyme-linked immunosorbent assay (ELISA)

Cells were seeded onto 60-mm dishes. The conditioned medium was collected and obtained after the centrifugation at 1000 rpm for 2 min. The transforming growth factor (TGF)-β levels of the media were measured with commercially available ELISA kits (R&D Systems Inc., Minneapolis, MN).

Cytokine treatment

Here, we used sham-operated BALB/cJ mice cells as a control. One hundred thousand cells were seeded onto 35-mm tissue culture dishes and cultured. After 4 h seeding in a 5% CO_2 atmosphere at 37°C, cells were treated with TGF-β1 (0, 2, and 10 ng/mL). Thereafter, SLDT and RT-PCR were performed. Purified human TGF-β1 was purchased from R&D Systems.

Statistical analysis

Student *t* test was used to compare the implanted samples with the controls. Statistical significance was accepted at $p < 0.05$. Values were presented as the mean ± standard deviation.

RESULTS AND DISCUSSION

There are many known tumorigenesis-inducing factors. It was reported that many plastics induce malignant tumors when implanted subcutaneously into rats and mice.[19–22] PLLA shows slow degradation, and therefore has been applied as a biomaterial for surgical devices such as bone plates, pins, and screws. It was reported in different studies that polyetherurethane, polyethylene, and PLLA produced tumors in rats.[6,7,23–25] In our study, tumors were induced by PLLA plates in BALB/cJ mice at 100% incidence but not in SJL/J mice at the surrounding tissues of PLLA plates during a 10-month *in vivo* study. To understand the mechanisms of tumorigenesis induced by PLLA, we focused on the inhibitory effects on GJIC at the early stage of tumorigenesis. To assess functional GJIC, the SLDT assay was performed. Brand et al.[26] reported that BALB/cJ mice are a higher and SJL/J mice are a lower tumorigenic strain. Our present results showed that the GJIC was significantly inhibited in 1-month PLLA-implanted BALB/cJ mice cells compared with BALB/cJ controls (Fig. 1). In contrast, no significant difference was observed between the 1-month PLLA-implanted SJL/J mice and SJL/J controls (Fig. 1). The data also revealed that the dye migration was higher in control BALB/cJ mice than control SJL/J mice (Fig. 1). High responder to the tumorigenicity may be classified as animals that are easily suppressed in both GJIC function and the connexins expression. This perturbed gap junction is likely to have a major role in the PLLA-induced tumorigenesis. Gap junctions are also regulated by the posttranslational phosphorylation of the carboxy-terminal tail region on the connexin molecule. Phosphorylation of connexin molecules is closely related with the inhibition of GJIC.[27,28] Phosphorylation has been involved in controlling a broad variety of connexin processes that include trafficking, gathering/nongathering, degradation, and also the gating of gap channels. It was also reported that communication-deficient cells did not express the Cx43–biphosphorylated (P_2) isoform but cells with low gap-junction permeability showed detectable amounts of the Cx43–monophosphorylated (P_1) isoform.[16] To survey the cause, we examined the mRNA and protein expression of the Cx43 gene. Here, mRNA expression was suppressed in PLLA-implanted BALB/cJ mice compared with BALB/cJ controls [Fig. 2(A)]. No significant difference was observed between the PLLA-implanted SJL/J mice and SJL/J controls [Fig. 2(B)]. We also found that the total level of protein expression such as unphos-

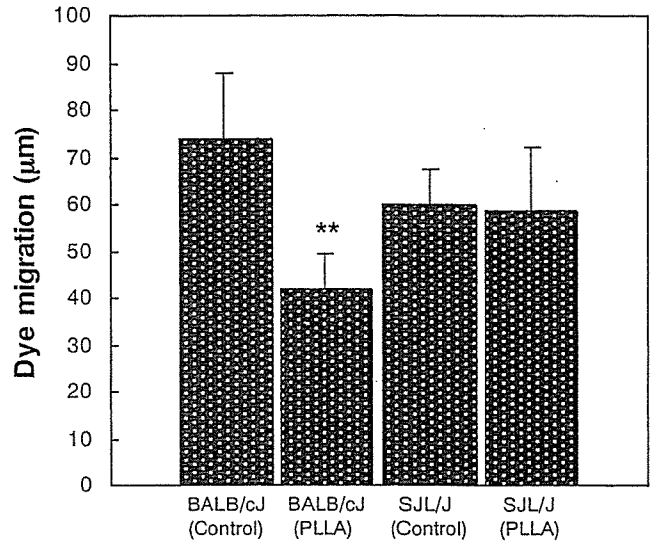

Figure 1. Statistical analysis of the SLDT assay. In both the implanted and sham-operated controls, three mice of each strain were sacrificed after 30 days. Results shown are representative of two independent experiments. GJIC was significantly inhibited in PLLA-implanted BALB/cJ mice cells compared with BALB/cJ controls. $^{**}p < 0.01$.

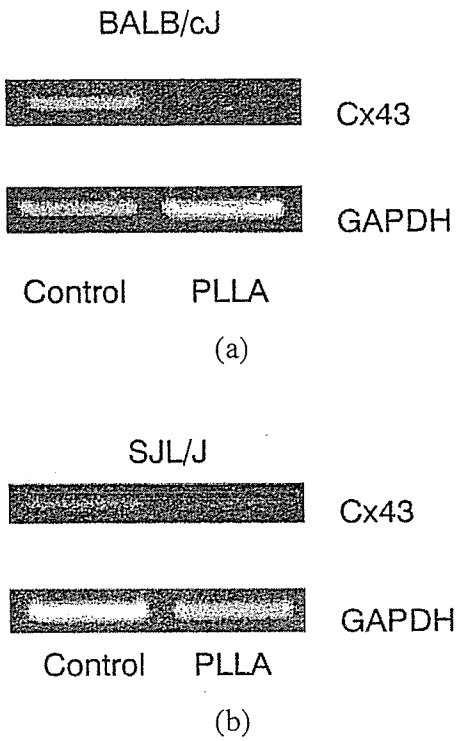

Figure 2. mRNA expression of Cx43 by RT-PCR analysis. In both the implanted and sham-operated controls, three mice of each strain were sacrificed after 30 days. Results shown are representative of two independent experiments. SYBR Green I stained PCR products after agarose gel electrophoresis showed that (A) mRNA expression was suppressed in PLLA-implanted BALB/cJ mice compared with BALB/cJ controls, and (B) no significant difference was observed between the PLLA-implanted SJL/J mice and SJL/J controls.

phorylated (P_0), P_1, and P_2 levels were significantly decreased in PLLA-implanted BALB/cJ mice compared with the control (Fig. 3). Asamoto et al.[29] reported that tumorigenicity was enhanced when the expression of Cx43 protein was suppressed by the anti-sense RNA of Cx43. A similar tendency was also observed in our study where the protein expression might be inhibited via down-regulation of the mRNA level. The genetic alteration and posttranslational

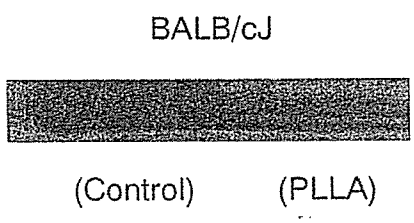

Figure 3. Protein expression of Cx43 by Western blot analysis. In both the implanted and sham-operated controls, three mice of each strain were sacrificed after 30 days. Results shown are representative of two independent experiments. Total level of protein expression such P_0, P_1, and P_2 levels were significantly decreased in PLLA-implanted BALB/cJ mice compared with the controls.

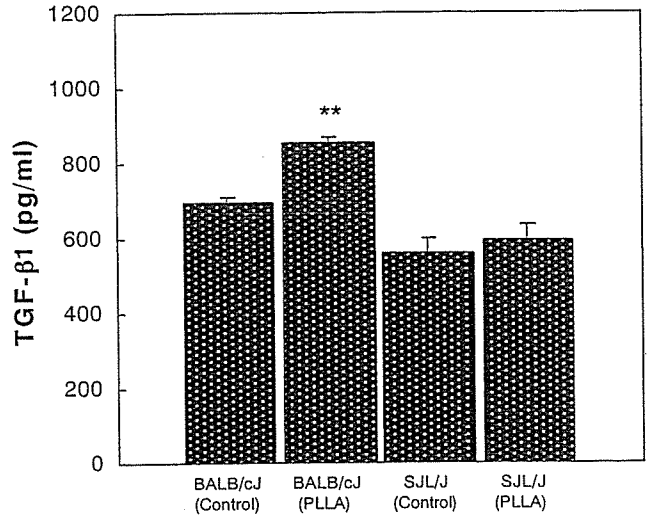

Figure 4. Statistical analysis of TGF-β1 cytokine assay by ELISA. In both the implanted and sham-operated controls, three mice of each strain were sacrificed after 30 days. Results shown are representative of two independent experiments. Secretion of the TGF-β1 level was significantly increased in PLLA-implanted BALB/cJ mice compared with BALB/cJ controls. $^{**}p < 0.01$.

modification in the Cx43 protein was shown to be involved in impaired GJIC and could be associated with tumorigenesis. Therefore, it is suggested that the inhibitory effect of PLLA on GJIC might be caused by the alteration in the Cx43 protein, causing enhancement of tumorigenesis. Moreover, Moorby and Patel[30] reported a direct action of the Cx43 protein on cell growth that was mediated via the cytoplasmic carboxyl domain.

Because TGF-β1 inhibits GJIC by decreasing the phosphorylated form of Cx43[31] and the phosphorylation of Cx43 has been implicated in gap-junction assembly and gating events,[16,27,32] we hypothesized that TGF-β1 might have an important role on PLLA-implanted BALB/cJ mice. Figure 4 clearly demonstrates that the secretion of the TGF-β1 level was significantly increased in PLLA-implanted BALB/cJ subcutaneous tissue in comparison with those from BALB/cJ control mice. No significant difference was found in the secretion of TGF-β1 between the SJL/J implanted and SJL/J control mice. TGF-β2 and TGF-β3 cytokine assay revealed no significant difference in TGF-β2 secretion and TGF-β3 was below the detection level (data not shown). So we performed an *in vitro* study, which showed that the intercellular communication and the mRNA expression of Cx43 were significantly suppressed in BALB/cJ control cells when treated with TGF-β1 [Fig. 5(A,B)].

In conclusion, we suggest that increased secretion of TGF-β1 (Fig. 4) suppressed expression of the gap-junctional protein Cx43 (Fig. 3) at the earlier stage after implantation of PLLA in BALB/cJ mice, resulting in

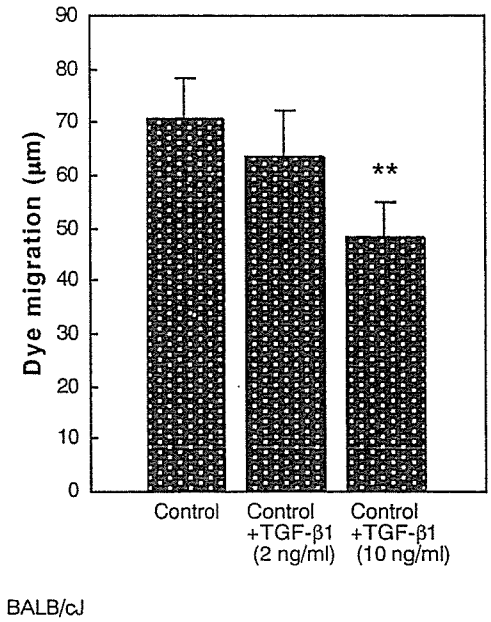

(a)

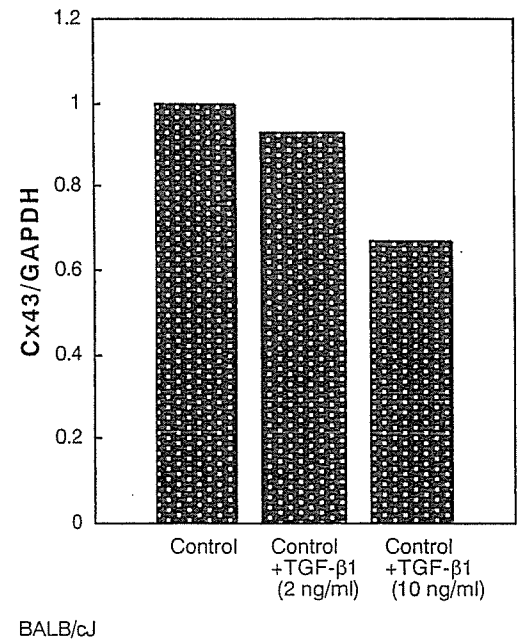

(b)

Figure 5. (A) SLDT assay. (B) National Institutes of Health image analysis quantitation of RT-PCR bands. In both figures, BALB/cJ control cells were treated with 2 and 10 ng/mL TGF-β1. GJIC was significantly inhibited and mRNA expression was significantly suppressed in BALB/cJ control cells treated with 10 ng/mL TGF-β1 compared with BALB/cJ controls. $^{**}p < 0.01$. Three dishes were used for one data point (bar) as one experiment. Results shown are representative of two independent experiments.

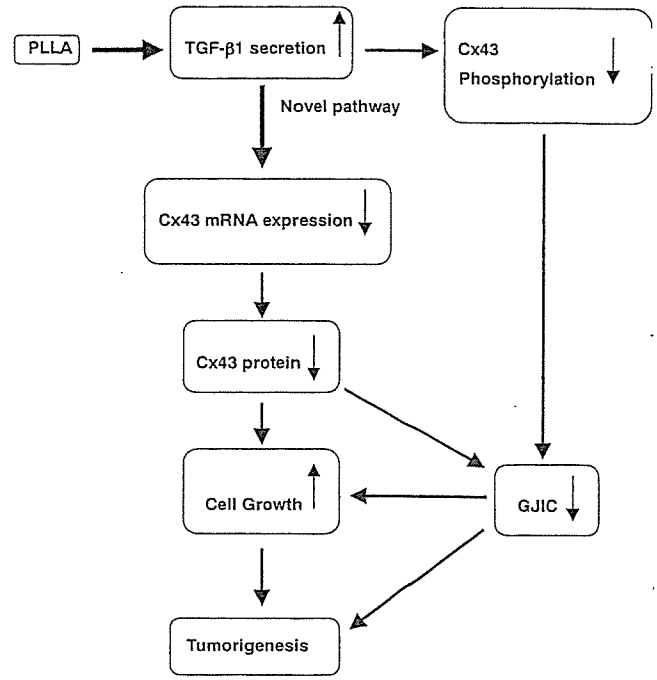

Figure 6. Schematic representation of the pathway of tumorigenesis induced by PLLA in BALB/cJ mice.

the suppression of the function of GJIC (Fig. 1) and at the same time, mRNA expression of Cx43 was suppressed in BALB/cJ mice (higher tumorigenic) but not in SJL/J mice (lower tumorigenic) [Fig. 2(A,B)]. TGF-β1 also suppressed the expression of mRNA of Cx43 and the function of GJIC in the BALB/cJ mouse cells *in vitro* [Fig. 5(A,B)]. These results indicated the novel mechanism of tumorigenesis induced by PLLA (Fig. 6).

References

1. Tang L, Eaton JW. Inflammatory responses to biomaterials. Am J Clin Pathol 1995;103:466–471.
2. Rames A, Williams DF. Immune response in biocompatibility. Biomaterials 1992;13:731–743.
3. Anderson JM. Mechanisms of inflammation and infection with implanted devices. Cardiovasc Pathol 1993;2:33s–41s.
4. Kulkarni RK, Pani KC, Neuman C, Leonard F. Polylactic acid for surgical implants. Arch Surg 1966;93:839–843.
5. Craig PH, Williams JA, Davis KW, Magoun AD, Levy AJ, Bogdansky S, Jones JP Jr. A biological comparison of polyglactin 910 and polyglycolic acid synthetic absorbable sutures. Surg Gynecol Obstet 1995;141:1–10.
6. Nakamura T, Shimizu Y, Okumura N, Matsui T, Hyon SH, Shimamoto T. Tumorigenicity of poly-L-lactide (PLLA) plates compared with medical-grade polyethylene. J Biomed Mater Res 1994;28:17–25.
7. Nakamura A, Kawasaki Y, Takada K, Aida Y, Kurokama Y, Kojima S, Shintani H, Matsui M, Nohmi T, Matsuoka A, Sofuni T, Kurihara M, Miyata N, Uchima T, Fujimaki M. Difference in tumor incidence and other tissue responses to polyetherurethanes and polydimethylsiloxane in long-term subcutaneous implantation into rats. J Biomed Mater Res 1992;26:631–650.

8. Trosko JE, Madhukar BV, Chang CC. Endogenous and exogenous modulation of gap junctional intercellular communication: toxicological and pharmacological implications. Life Sci 1993;53:1–19.
9. Trosko JE, Ruch RJ. Cell–cell communication in carcinogenesis. Front Biosci 1998;3:D208–236.
10. Eiberger J, Degen J, Romualdi A, Deutsch U, Willecke K, Sohl G. Connexin genes in the mouse and human genome. Cell Commun Adhes 2001;8:163–165.
11. Bruzzone R, White TW, Paul DL. Connections with connexins: the molecular basis of direct intercellular signaling. Eur J Biochem 1996;238:1–27.
12. Loewenstein WR. Junctional intercellular communication and the control of growth. Biochim Biophys Acta 1979;560:1–65.
13. Guthrie SC, Gilula NB. Gap junctional communication and development. Trends Neurosci 1989;12:12–16.
14. Klaunig JE, Ruch RJ. Role of inhibition of intercellular communication in carcinogenesis. Lab Invest 1990;62:135–146.
15. Mesnil M, Yamasaki H. Cell–cell communication and growth control of normal and cancer cells: evidence and hypothesis. Mol Carcinog 1993;7:14–17.
16. Musil LS, Goodenough DA. Biochemical analysis of connexin43 intracellular transport, phosphorylation, and assembly into gap junctional plaques. J Cell Biol 1991;115:1357–1374.
17. Musil LS, Goodenough DA. Multisubunit assembly of an integral plasma membrane channel protein, gap junction connexin43, occurs after exit from the ER. Cell 1993;74:1065–1077.
18. El-Fouly MH, Trosko JE, Chang CC. Scrape-loading and dye transfer. A rapid and simple technique to study gap junctional intercellular communication. Exp Cell Res 1987;168:422–430.
19. Turner FC. Sarcomas at sites of subcutaneously implanted bakelite disks in rats. J Natl Cancer Inst 1941;2:81–83.
20. Oppenheimer BS, Oppenheimer ET, Danishefsky I, Stout AP, Eirich FR. Further studies of polymers as carcinogenic agents in animals. Cancer Res 1955;15:333–340.
21. Bischoff F, Bryson G. Carcinogenesis through solid state surface. Prog Exp Tumor Res 1964;5:85–133.
22. Karp RD. Tumorigenesis by Millipore filters in mice: histology and ultrastructure of tissue reactions as related to pore size. J Natl Cancer Inst 1973;51:1275–1285.
23. Tsuchiya T, Hata H, Nakamura A. Studies on the tumor-promoting activity of biomaterials: inhibition of metabolic cooperation by polyetherurethane and silicone. J Biomed Mater Res 1995;29:113–119.
24. Tsuchiya T. A useful marker for evaluating tissue-engineered products: gap-junctional communication for assessment of the tumor-promoting action and disruption of cell differentiation in tissue-engineered products. J Biomater Sci Polym Ed 2000; 11:947–959.
25. Nakaoka R, Tsuchiya T, Kato K, Ikada Y, Nakamura A. Studies on tumor-promoting activity of polyethylene: inhibitory activity of metabolic cooperation on polyethylene surfaces is markedly decreased by surface modification with collagen but not with RGDS peptide. J Biomed Mater Res 1997;35:391–397.
26. Brand I, Buoen LC, Brand KG. Foreign-body tumors of mice: strain and sex differences in latency and incidence. J Natl Cancer Inst 1977;58:1443–1447.
27. Musil LS, Cunningham BA, Edelman GM, Goodenough DA. Differential phosphorylation of the gap junction protein connexin43 in junctional communication-competent and -deficient cell lines. J Cell Biol 1990;111:2077–2088.
28. Lampe PD, Lau AF. Regulation of gap junctions by phosphorylation of connexins. Arch Biochem Biophys 2000;384:205–215.
29. Asamoto M, Toriyama-Baba T, Krutovskikh V, Cohen SM, Tsuda H. Enhanced tumorigenicity of rat bladder squamous cell carcinoma cells after abrogation of gap junctional intercellular communication. Jpn J Cancer Res 1998;89:481–486.
30. Moorby C, Patel M. Dual functions for connexins: Cx43 regulates growth independently of gap junction formation. Exp Cell Res 2001;271:238–248.
31. Wyatt LE, Chung CY, Carlsen B, Iida-Klein A, Rudkin GH, Ishida K, Yamaguchi DT, Miller TA. Bone morphogenetic protein-2 (BMP-2) and transforming growth factor-beta1 (TGF-beta1) alter connexin 43 phosphorylation in MC3T3-E1 cells. BMC Cell Biol 2001;2:14.
32. Laird DW, Castillo M, Kasprzak L. Gap junction turnover, intracellular trafficking, and phosphorylation of connexin43 in brefeldin A-treated rat mammary tumor cells. J Cell Biol 1995; 131:1193–1203.

Available online at www.sciencedirect.com
SCIENCE DIRECT®
Neuroscience Letters 370 (2004) 155–159
Neuroscience Letters
www.elsevier.com/locate/neulet

4-Hydroxynonenal modulates the long-term potentiation induced by L-type Ca^{2+} channel activation in the rat dentate gyrus in vitro

Tatsuhiro Akaishi[a,b], Ken Nakazawa[b], Kaoru Sato[b], Yasuo Ohno[b], Yoshihisa Ito[a,*]

[a] *Department of Pharmacology, College of Pharmacy, Nihon University, 7-7-1 Narashinodai, Funabashi-shi, Chiba 274-8555, Japan*
[b] *Division of Pharmacology, National Institute of Health Sciences, Setagaya-ku, Tokyo 158-8501, Japan*

Received 15 June 2004; received in revised form 23 July 2004; accepted 8 August 2004

Abstract

Increased oxyradical production and membrane lipid peroxidation (MLP) occur under physiological and degenerative conditions in neurons. We investigated whether 4-hydroxynonenal (4HN), one of the membrane lipid peroxidation products, affects long-term potentiation (LTP) in the rat dentate gyrus in vitro. Treatment of hippocampal slices with 4HN (10 μM) enhanced LTP without affecting basal evoked potentials. The enhancement was completely inhibited by 2 μM nifedipine, a blocker of L-type Ca^{2+} channels. In cultured dentate gyrus neurons, treatment of the cells with 4HN for 24 h resulted in a significant amount of cell death that was detoxified by glutathione, whereas short-term treatment with 4HN (≦6 h) had no effect. Nifedipine partially but significantly suppressed the 4HN-induced cell death. These results suggest that 4HN modulates LTP and induces delayed cell death through L-type Ca^{2+} channel activation in the dentate gyrus. 4HN thereby plays an important role in both physiological and pathophysiological events in the hippocampus.

Keywords: 4-Hydroxynonenal; Oxidative stress; Long-term potentiation; Ca^{2+} channel; Hippocampus; Dentate gyrus

Oxidative stress is implicated in a variety of physiological and pathophysiological processes such as immune defense, ischemia, and neurodegenerative diseases (e.g., Alzheimer's disease, AD) [7,8,17,23]. It has been shown that levels of membrane lipid peroxidation (MLP) and thiobarbituric-acid-reactive substances are elevated in AD brains [16,18]. Several reports have shown that one of the MLP products, 4-hydroxynonenal (4HN), is generated in response to oxidative insults and is found in association with many different neurodegenerative diseases, such as AD [14,17], Parkinson's disease [24], and sporadic amyotrophic lateral sclerosis [22]. We have recently reported that oxidative stress affects the activity of voltage-gated Ca^{2+} channels (VGCCs), and that the currents through VGCCs are significantly increased by treatment with 4HN in cultured dentate granule cells [1,2]. These results suggest that 4HN activates VGCCs in the dentate granule cells, and that this action is linked to both physiological and pathophysiological events.

Long-term potentiation (LTP) in the hippocampus is a form of synaptic plasticity and is thought to be one of the cellular mechanisms underlying learning and memory. LTP is induced by high-frequency stimulation (HFS), and it requires activation of *N*-methyl-d-aspartate (NMDA) receptors and consequent Ca^{2+} entry into the postsynaptic neurons at least in area CA1 of the hippocampus and the dentate gyrus [5]. Recent studies have demonstrated that not only Ca^{2+} influx through NMDA receptors, but also that through VGCCs or store-operated Ca^{2+} channels play important roles in the induction or regulation of LTP [4,6]. Recently, a link between oxidative stress and modulation of synaptic plasticity has been proposed. It has been demonstrated that physiologically relevant concentrations of hydrogen peroxide (H_2O_2), a membrane-permeable form of reactive oxygen species, modify synaptic plasticity in the hippocampal CA1 region in rats [13]. However, the involvement of 4HN in synaptic plasticity in the hippocampus has yet to be elucidated. To address this

* Corresponding author. Tel.: +81 474 65 5832; fax: +81 474 65 5832.
E-mail address: yoshiito@pha.nihon-u.ac.jp (Y. Ito).

0304-3940/$ – see front matter © 2004 Elsevier Ireland Ltd. All rights reserved.
doi:10.1016/j.neulet.2004.08.015

point, in the present study, the effects of 4HN on LTP in the rat dentate gyrus were examined in vitro. We found that 4HN modulates LTP via the activation of L-type VGCCs, and that long-term exposure of cultured dentate granule cells to 4HN induces neuronal death, at least in part, through mechanisms involving a VGCC-mediated pathway.

All procedures in this study were carried out in accordance with the guidelines of the National Institutes of Health Sciences. Preparation of hippocampal slices and recording of evoked potentials were done as described in our previous papers [3,12]. In brief, hippocampal slices (400 μm thick) were prepared from male Wistar rats (4–6 weeks old) and maintained in a chamber at 30 °C, where they were continuously perfused with oxygenated (95% O_2:5% CO_2) artificial cerebrospinal fluid (ACSF). The composition of the ACSF was as follows (in mM): 124 NaCl, 1.25 NaH_2PO_4, 2.5 KCl, 2.0 $CaCl_2$, 1.0 $MgCl_2$, 26.0 $NaHCO_3$, and 10.0 glucose. The perforant path was stimulated with a bipolar tungsten electrode, and the evoked potential was recorded extracellularly from the granule cell layer of the dentate gyrus with a glass capillary microelectrode filled with 2 M NaCl (tip resistance 2–8 MΩ). Single-pulse test stimulations (0.1 ms duration) were applied at 30-s intervals. The stimulus intensity was adjusted to produce synaptic potential amplitudes that were of 50% of the maximum.

Dentate gyrus neurons in the hippocampus were obtained from 3- to 4-day-old Wistar rats and enzymatically dissociated as described previously [1,2]. The cells were suspended in a mixture of 50% Neurobasal medium containing 2% B-27 supplement, 73 μg/ml l-glutamine, and 50% astrocyte-conditioned medium (ACM). The cells were plated on polyethyleneimine-coated 96-well plates (20,000 cells/cm^2). The ACM-containing medium was changed to an ACM-free medium 1 day after the plating. The culture medium was changed twice a week thereafter. At days 7–8, the medium was removed and replaced with Locke's solution (154 mM NaCl, 5.6 mM KCl, 2.3 mM $CaCl_2$, 1.0 mM $MgCl_2$, 3.6 mM $NaHCO_3$, 10 mM glucose, and 5 mM 4-(2-hydroxyethyl)-1-piperazineethanesulfonic acid; pH 7.2). The effects of 4HN on LTP or cell viability were investigated using drugs added to ACSF or Locke's solution, respectively. 4HN (Cayman Chemical, Ann arbor, MI, U.S.A.) and nifedipine (Sigma, St Louis, MO, U.S.A.) were prepared as 1000× and 500× stock solutions, respectively in ethanol. Glutathione (GSH)-ethyl ester (Sigma) was prepared as a 100× stock solution in saline. Cell viability was evaluated by the 3-(4,5-dimethythiazol-2-yl)-2,5-diphenyltetrazolium bromide (MTT) reduction assay, as described previously [11,14].

To evaluate changes in evoked potentials, the amplitude of the population spike (PS) was measured as described in our previous reports [3,12]. When 10 μM 4HN was applied to the slices, there was no change in PS amplitude (Fig. 1A), suggesting that 4HN does not affect basal evoked potentials in the dentate gurus. We next investigated effects of 4HN on LTP in the dentate gyrus. In control slices, the application of HFS produced a robust potentiation of the PS that

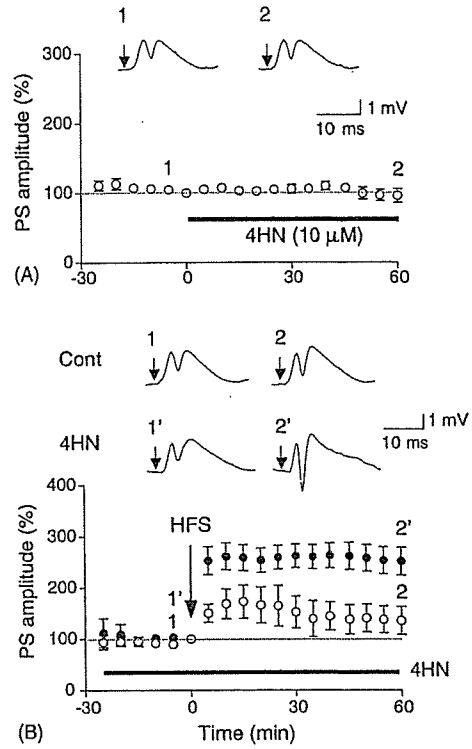

Fig. 1. Effects of 4HN on basal evoked potentials and LTP in the dentate gyrus in vitro. (A) Time-course of changes in basal evoked potentials ($n = 4$). Hippocampal slices were treated with 4HN (10 μM) for 60 min (0–60 min), and evoked potentials were observed without applying HFS. (B) Time-course of LTP induced in the absence (open circles, $n = 4$) or presence (closed circles, $n = 6$) of 4HN (10 μM). HFS (100 pulses at 100 Hz) was applied at time 0. The amplitude of the evoked potentials is expressed as a percentage of the baseline value (at time 0), which was recorded immediately before the application of 4HN (A) or HFS (B). Insets are representative records of evoked potentials at the times denoted by the numbers. A test stimulation was delivered at the times indicated by arrows. All data are presented as the mean ± S.E.M.

lasted for 60 min and reached approximately 140% of the basal level (Fig. 1B, open circles). When hippocampal slices were pretreated with 10 μM 4HN for 1 h, the degree of LTP that was then induced was larger than in the control group (Fig. 1B). The mean amplitude of PS of 30–60 min after HFS was 139.1 ± 28.6% in the control group and 258.0 ± 25.5% in the 4HN-treated group. We have shown recently, using the whole cell patch clamp technique, that 4HN selectively activates L-type VGCCs in dentate granule cells [2]. In order to examine whether VGCCs contribute to the 4HN-induced enhancement of LTP, we investigated the effects of nifedipine, an L-type VGCC blocker. In our preliminary experiment, exposure of slices to nifedipine (2 μM) alone did not affect LTP ($n = 4$, data not shown). As shown in Fig. 2, the 4HN-induced enhancement of LTP was completely blocked when slices were treated with 2 μM nifedipine. These results suggest that 4HN enhances LTP in the dentate gyrus, and that this enhancement is attributable to the activation of L-type VGCCs.

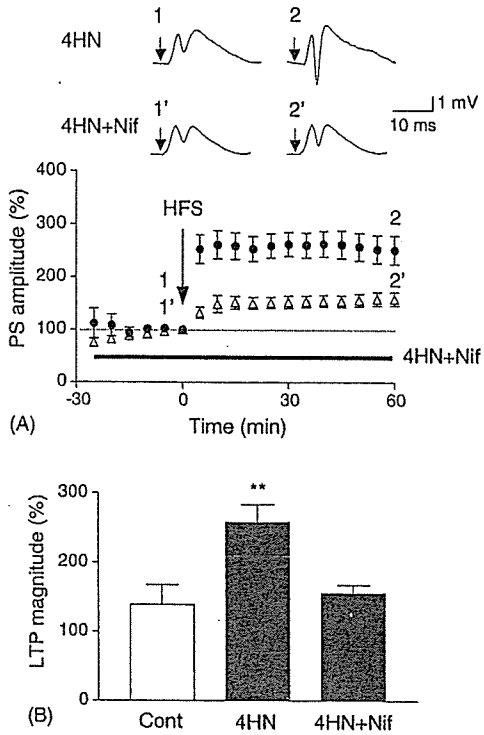

Fig. 2. Effects of nifedipine (Nif) on the enhancement of LTP in the dentate gyrus in vitro. (A) Time-course of changes in evoked potentials. Hippocampal slices were treated with 4HN (10 μM) in the presence or absence of Nif (2 μM) for 1 h, and then HFS was applied at time 0 (open triangles, $n = 6$). The amplitude of the evoked potentials is expressed as a percentage of the baseline value, which was recorded immediately before the onset of HFS (time 0). Insets are representative records of evoked potentials at the times denoted by the numbers. A test stimulation was delivered at the times indicated by arrows. To allow a direct comparison, the 4HN-treated data (the same data as Fig. 1B) are superimposed. (B) Comparison of LTP magnitude among the three groups (control group, Cont; 4HN-treated group, 4HN; 4HN- and Nif-cotreated group, 4HN + Nif). The average of evoked potential amplitudes 30–60 min after HFS was calculated as an index of LTP magnitude. Values are given as the mean ± S.E.M. $^{**}P < 0.01$ vs. Cont, Dunnett's test.

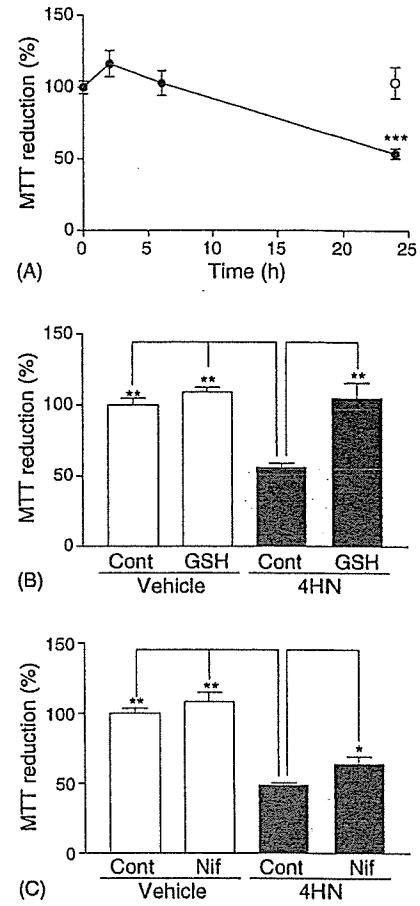

Fig. 3. 4HN induces delayed cell death in dentate gyrus neurons, but this effect is inhibited by simultaneous treatment with either GSH or Nif. (A) Time-course of changes in 4HN-induced cell death. 4HN (10 μM) was applied at time 0, and levels of MTT reduction were examined at the time point indicated (closed circles, $n = 6$–8). To enable a direct comparison, the vehicle (0.02% ethanol)-treated cells are shown as ○ ($n = 7$). GSH-ethyl ester (1 mM) blocked (B, $n = 7$–9), and Nif (2 μM) attenuated (C, $n = 10$–14) the delayed cell death induced by 4HN. Cells were exposed to the indicated agents, and neuronal survival was quantified. Values are presented as the mean ± S.E.M. $^{***}P < 0.001$ vs. the vehicle, Student's t-test. $^{*}P < 0.05$; $^{**}P < 0.01$ vs. 4HN (Cont), Dunnett's test.

There is a growing body of evidence to suggest that prolonged exposure of hippocampal neurons to 4HN results in delayed cell death [10,14,15]. Therefore, we also examined the effects of 4HN on cell viability using primary dentate gyrus neurons. The time course of 4HN-induced toxicity is shown in Fig. 3A. Exposure of the cells to 10 μM 4HN resulted in no decrease in the levels of MTT reduction during the first 6 h. In contrast, a significant decrease in MTT levels was observed at 24 h following the application of 4HN (53.9% of basal levels). The level of MTT reduction in the 4HN-treated groups was significantly lower than in the vehicle-treated groups (Fig. 3A). GSH is a covalent modifier of 4HN and can thereby detoxify 4HN [1,15]. We examined the effects of GSH-ethyl ester, a membrane-permeable form of GSH, on 4HN-induced cell death. As shown in Fig. 3B, the 4HN-induced cell death was completely blocked when cells were treated with 1 mM GSH-ethyl ester. In addition, nifedipine (2 μM) partially but significantly attenuated 4HN-induced cell death (Fig. 3C), indicating that Ca^{2+} influx through VGCCs, at least in part, underlies the cell death.

The data presented here demonstrate that 10 μM 4HN significantly enhances LTP without affecting basal evoked potentials in the dentate gyrus, and that this enhancement is completely blocked when slices are treated with 2 μM nifedipine. These findings suggest that Ca^{2+} influx through the L-type VGCCs plays a pivotal role in synaptic plasticity in certain conditions in the dentate gyrus. To our knowledge, this is the first report to provide direct evidence that 4HN modulates LTP via the activation of L-type VGCCs. However, it

remains to be elucidated whether the 4HN-induced enhancement of LTP is involved in physiological and/or pathophysiological phenomena.

In general, MLP products are thought to be involved in certain types of neurodegenerative disorders. For example, levels of 4HN are increased in association with the neurodegenerative process in postmortem tissue samples from patients with AD [16]. Studies of experimental models of AD suggested a pivotal role for 4HN in the neurodegenerative process [11,14,15]. It has been reported that age-related changes in the levels of MLP in the hippocampus are associated with alterations in the level of LTP in the dentate gyrus [19]. On the other hand, there are recent indications supporting the involvement of MLP in physiological phenomena. It has been reported that levels of MLP increase in response to stimuli that induce LTP [21]. Kamsler and Segal [13] demonstrated that a physiologically relevant concentration (1 μM) of H_2O_2 increased LTP and suppressed long-term depression, while higher concentrations (0.5–5 mM) of H_2O_2 suppressed basal synaptic transmission in the rat hippocampus. In our previous experiments using the whole cell patch clamp technique, we demonstrated that low concentrations (1 and 10 μM) of H_2O_2 and 4HN selectively modulate L-type VGCCs in cultured dentate granule cells [1,2]. Because it has been already shown that VGCCs are involved in various physiological functions in neurons [9,20], the action of 4HN as well as H_2O_2 may be implicated not only in pathophysiological phenomena but also in physiological events in the hippocampus. In the present study, we used a concentration of 10 μM throughout the electrophysiological experiments because 10 μM 4HN showed a robust and significant VGCC-enhancing effect in our previous report [2]. Further detailed investigations using various concentrations of 4HN will be necessary to elucidate the relevance of 4HN to physiological phenomena in the hippocampus.

In the present study, we have also demonstrated that long-term exposure of cultured dentate gyrus neurons to 4HN, at a concentration that is known to modulate the activity of L-type VGCCs [2], results in a decrease of cell viability. It is not clear, at present, how long-term exposure to 4HN could induce cell death in these neurons. A possible explanation is that excessive Ca^{2+} influx through VGCCs contributes to neuronal death, although these channels are also involved in various physiological functions in these neurons. Long-term exposure of 4HN may switch on arrays of toxic events through excessive Ca^{2+} influx, while its short-term exposure may lead to physiological functions including the enhancement of LTP.

The exact mechanisms whereby 4HN modulates the VGCCs activity in neurons remain to be elucidated. In our preliminary studies, enhancement of Ca^{2+} current by 4HN requires a lag time period of about 1 h to become evident. The modulatory effect of 4HN on LTP and cell death, as shown in the present study, may be mediated through several kinase- or phosphatase-dependent pathways.

Acknowledgments

This work was partly supported by Health and Labour Science Research Grants for Research on Advanced Medical Technology from the Ministry of Health, Labour, and Welfare, Japan, a Grant-in-aid for Scientific Research from the Ministry of Education, Culture, Sports, Science, and Technology, Japan (KAKENHI 13672319) awarded to K.N., and a Grant-in-aid for Young Scientists from the Ministry of Education, Science, Sports, and Culture, Japan (KAKENHI 15700280) awarded to K.S.

References

[1] T. Akaishi, K. Nakazawa, K. Sato, H. Saito, Y. Ohno, Y. Ito, Hydrogen peroxide modulates whole cell Ca^{2+} currents through L-type channels in cultured rat dentate granule cells, Neurosci. Lett. 356 (2004) 25–28.

[2] T. Akaishi, K. Nakazawa, K. Sato, H. Saito, Y. Ohno, Y. Ito, Modulation of voltage-gated Ca^{2+} current by 4-hydroxynonenal in dentate granule cells, Biol. Pharm. Bull. 27 (2004) 174–179.

[3] T. Akaishi, H. Saito, Y. Ito, K. Ishige, Y. Ikegaya, Morphine augments excitatory synaptic transmission in the dentate gyrus through GABAergic disinhibition, Neurosci. Res. 38 (2000) 357–363.

[4] A. Baba, T. Yasui, S. Fujisawa, R.X. Yamada, M.K. Yamada, N. Nishiyama, N. Matsuki, Y. Ikegaya, Activity-evoked capacitative Ca^{2+} entry: implications in synaptic plasticity, J. Neurosci. 23 (2003) 7737–7741.

[5] T.V.P. Bliss, G.L. Collingridge, A synaptic model of memory: long-term potentiation in the hippocampus, Nature 361 (1993) 31–39.

[6] L.M. Grover, T.J. Teyler, Two components of long-term potentiation induced by different patterns of afferent activation, Nature 347 (1990) 477–479.

[7] K. Ishige, Q. Chen, Y. Sagara, D. Schubert, The activation of dopamine D4 receptors inhibits oxidative stress-induced nerve cell death, J. Neurosci. 21 (2001) 6069–6076.

[8] K. Ishige, D. Schubert, Y. Sagara, Flavonoids protect neuronal cells from oxidative stress by three distinct mechanisms, Free Radic. Biol. Med. 30 (2001) 433–446.

[9] K. Ito, K. Nakazawa, S. Koizumi, M. Liu, K. Takeuchi, T. Hashimoto, Y. Ohno, K. Inoue, Inhibition by antipsychotic drugs of L-type Ca^{2+} channel current in PC1 cells, Eur. J. Pharmacol. 314 (1996) 143–150.

[10] Y. Ito, M. Arakawa, K. Ishige, H. Fukuda, Comparative study of survival signal withdrawal- and 4-hydroxynonenal-induced cell death in cerebellar granule cells, Neurosci. Res. 35 (1999) 321–327.

[11] Y. Ito, Y. Kosuge, T. Sakikubo, K. Horie, N. Ishikawa, N. Obokata, E. Yokoyama, K. Yamashina, M. Yamamoto, H. Saito, M. Arakawa, K. Ishige, Protective effect of *S*-allyl-l-cysteine, a garlic compound, on amyloid β-protein-induced cell death in nerve growth factor-differentiated PC12 cells, Neurosci. Res. 46 (2003) 119–125.

[12] Y. Ito, K. Tabata, M. Makimura, H. Fukuda, Acute and chronic intracerebroventricular morphine infusions affect long-term potentiation differently in the lateral perforant path, Pharmacol. Biochem. Behav. 70 (2001) 353–358.

[13] A. Kamsler, M. Segal, Hydrogen peroxide modulation of synaptic plasticity, J. Neurosci. 23 (2003) 269–276.

[14] Y. Kosuge, Y. Koen, K. Ishige, K. Minami, H. Urasawa, H. Saito, Y. Ito, *S*-Allyl-l-cysteine selectively protects cultured rat hippocampal neurons from amyloid β-protein- and tunicamycin-induced neuronal death, Neuroscience 122 (2003) 885–895.

[15] I. Kruman, A.J. Bruce-Keller, D. Bredesen, G. Waeg, M.P. Mattson, Evidence that 4-hydroxynonenal mediates oxidative stress-induced neuronal apoptosis, J. Neurosci. 17 (1997) 5089–5100.
[16] M.A. Lovell, W.D. Ehmann, M.P. Mattson, W.R. Markesbery, Elevated 4-hydroxynonenal in ventricular fluid in Alzheimer's disease, Neurobiol. Aging 18 (1997) 457–461.
[17] R.J. Mark, E.M. Blanc, M.P. Mattson, Amyloid β-peptide and oxidative cellular injury in Alzheimer's disease, Mol. Neurobiol. 12 (1996) 211–224.
[18] S. Miranda, C. Opazo, L.F. Larrondo, F.J. Munoz, F. Ruiz, F. Leighton, N.C. Inestrosa, The role of oxidative stress in the toxicity induced by amyloid β-peptide in Alzheimer's disease, Prog. Neurobiol. 62 (2000) 633–648.
[19] C.A. Murray, M.A. Lynch, Dietary supplementation with vitamin E reverses the age-related deficit in long-term potentiation in dentate gyrus, J. Biol. Chem. 273 (1998) 12161–12168.
[20] Y. Niikura, K. Abe, M. Misawa, Involvement of L-type Ca^{2+} channels in the induction of long-term potentiation in the basolateral amygdala-dentate gyrus pathway of anesthetized rats, Brain Res. 1017 (2004) 218–221.
[21] N.S. Nilova, L.N. Polezhaeva, Peroxidative oxidation of lipids in slices of olfactory cortex of the rat brain during long-term potentiation, Neurosci. Behav. Physiol. 26 (1996) 23–26.
[22] W.A. Pedersen, W. Fu, J.N. Keller, W.R. Markesbery, S. Appel, R.G. Smith, E. Kasarskis, M.P. Mattson, Protein modification by the lipid peroxidation product 4-hydroxynonenal in the spinal cords of amyotrophic lateral sclerosis patients, Ann. Neurol. 44 (1998) 819–824.
[23] Y. Sagara, K. Ishige, C. Tsai, P. Maher, Tyrphostins protect neuronal cells from oxidative stress, J. Biol. Chem. 277 (2002) 36204–36215.
[24] A. Yoritaka, N. Hattori, K. Uchida, M. Tanaka, E.R. Stadtman, Y. Mizuno, Immunohistochemical detection of 4-hydroxynonenal protein adducts in Parkinson disease, Proc. Natl. Acad. Sci. U.S.A. 93 (1996) 2696–2701.

Highlighted paper selected by Editor-in-chief

Modulation of Voltage-Gated Ca^{2+} Current by 4-Hydroxynonenal in Dentate Granule Cells

Tatsuhiro AKAISHI,[a,b] Ken NAKAZAWA,[b] Kaoru SATO,[b] Hiroshi SAITO,[a] Yasuo OHNO,[b] and Yoshihisa ITO*,[a]

[a] *Department of Pharmacology, College of Pharmacy, Nihon University; Funabashi 274–8555, Japan: and* [b] *Division of Pharmacology, National Institute of Health Sciences; Setagaya-ku, Tokyo 158–8501, Japan.*

Received October 11, 2003; accepted December 4, 2003; published online December 12, 2003

Although recent studies have suggested that dentate granule cells play a key role in hippocampal functions, electrophysiological properties in these cells have not been sufficiently explored. In the present study, modification of voltage-gated Ca^{2+} channels by 4-hydroxynonenal (4HN), a major aldehydic product of membrane lipid peroxidation, in cultured dentate granule cells was examined using the whole-cell patch clamp technique. When whole-cell voltage clamp was applied, the cells exhibited a high-voltage-activated Ca^{2+} current, which was totally sensitive to 30 μM Cd^{2+} and partially sensitive to 2 μM nifedipine. 4HN enhanced the Ca^{2+} current in these cells. When L-type Ca^{2+} channels were blocked by application of nifedipine, the enhancement was completely canceled, whereas application of ω-conotoxin-GVIA or ω-agatoxin-IVA, blockers of N- and P/Q-type Ca^{2+} channels, respectively, had no effect. These results suggest that 4HN modulates L-type Ca^{2+} channels in the dentate granule cells, and thereby plays a role in the physiological and pathophysiological responses of these cells to oxidative stress.

Key words dentate granule cell; Ca^{2+} channel; 4-hydroxynonenal; hippocampus

The formation of the hippocampus appears to be essential for certain forms of learning and memory. Several studies have suggested that dentate granule cells play important roles in associative learning.[1—3] Destruction of dentate granule cells with colchicine, or their selective loss following long-term adrenalectomy causes spatial memory deficits and impairments in several learning tasks.[1—3] This memory deficit has been shown to correlate with a loss of dentate granule cells. The dentate gyrus is known to be one of the few regions in the adult mammalian brain that exhibit ongoing neurogenesis. The production of dentate granule cells occurs continuously, even after birth. Their precursors divide in the subgranular proliferative zone at the border of the granule cell layer and the hilus. A proportion of the newborn cells differentiate into neurons, migrate into the granule cell layer, and project to the CA3 region of the hippocampus. Several lines of evidence have suggested that newly generated granule cells play a role in cognition and brain repair.[2,4,5] Furthermore, it has already been reported that cultured dentate granule cells provide a faithful and useful model of mossy fiber sprouting.[6]

Although dentate granule cells play important roles in hippocampal functions, the electrophysiological properties of these cells have not been clarified sufficiently. Both *in situ* hybridization and immunocytochemical experiments have demonstrated that the level of L-type Ca^{2+} channel subunit expression is higher in the dentate granule cell layer than in any other area of the hippocampus.[7] Thus, it is very important to characterize in detail the Ca^{2+} currents that arise through voltage-gated Ca^{2+} channels (VGCCs) in dentate granule cells if we are to understand their physiological and pathological relevance.

Oxidative stress is implicated in a variety of physiological and pathophysiological processes such as immune defense, ischemia, and neurodegenerative diseases (*e.g.*, Alzheimer's disease, AD).[8—11] Oxidative stress arising from excessive production or decreased clearance of reactive oxygen species (ROS) can result in the accumulation of ROS, cellular damage, and eventual cell death. Indeed, the molecular and cellular events underlying the neuronal death induced by oxidative stress have been clarified in the HT-22 hippocampal cell line and in cortical neurons.[12—14]

Levels of lipid peroxidation are increased in the brain of AD patients, and the levels of thiobarbituric-acid-reactive substances are elevated in most regions of the AD brain compared with controls.[15] One of the lipid peroxidation products, 4-hydroxynonenal (4HN), has been shown to play important roles in the neuronal cell death associated with many different neurodegenerative diseases, such as AD,[8,9] Parkinson's disease,[16] and sporadic amyotrophic lateral sclerosis.[17] Several studies have shown that 4HN is generated in response to oxidative insults and can induce neuronal apoptosis.[18—20] Furthermore, it has been demonstrated that the mechanisms underlying the neuronal damage induced by 4HN involves the disturbance of ion homeostasis.[9] Despite the importance of 4HN-induced neuronal damage, the modulation of Ca^{2+}-channel activity by 4HN has not been adequately studied in dentate granule cells.

In order to clarify this issue, we employed a dissociated cell culture system of dentate granule cells, the whole-cell patch clamp technique, characterized the properties of the Ca^{2+} current in dentate granule cells, and investigated whether and how 4HN could affect the current in these cells.

MATERIALS AND METHODS

All experiments in this study were performed in accordance with the guidelines of the National Institute of Health Sciences.

Cell Culture Unless otherwise specified, neurons were cultivated in Neurobasal medium (Life Technologies, Gaithersburg, MD, U.S.A.) supplemented with 73 μg/ml L-

* To whom correspondence should be addressed. e-mail: yoshiito@pha.nihon-u.ac.jp

glutamine (Wako, Osaka, Japan) and 2% B-27 supplement (Life Technologies). Three- to 4-d-old Wistar rat pups (Nihon SLC, Shizuoka, Japan) were deeply anesthetized with ether, and the hippocampi were removed. The dentate gyrus was dissociated from the hippocampus with extreme care and under visual control. The dentate gyrus was cut into pieces, which were then treated with 0.25% trypsin (Difco, Detroit, MI, U.S.A.) and 0.01% deoxyribonuclease I (Sigma, St Louis, MO, U.S.A.) at 37 °C for 30 min. The incubation was terminated by addition of heat-inactivated horse serum (HS; Cell Culture, Cleveland, OH, U.S.A.). The tissue fragments were centrifuged at 1200 rpm for 5 min. The supernatant was removed and the pellet was suspended in a mixture of 50% Neurobasal medium/B-27 supplement and 50% astrocyte-conditioned medium (ACM), which was prepared according to Ikegaya *et al.*[6] In general, cultured astrocytes are known to posses a range of neurotrophic activities in culture and have been found to express mRNA for neurotrophic factors such as ciliary neurotrophic factor, nerve growth factor, and neurotrophin 3.[21] The suspension was gently triturated until visibly dispersed, and then filtered through a nylon net. The cells were plated at a density of 2.0×10^4 cells/cm^2 onto round, 13-mm-diameter glass cover slips (Matsunami, Osaka, Japan) that had been coated with polyethyleneimine (Sigma). In order to support the adhesion and survival of neurons, we used the culture medium containing ACM for 24 h after the plating. The culture medium was changed to ACM-free Neurobasal/B-27 medium thereafter. The cultures were maintained in the same medium at 37 °C in a humidified incubator with 5% CO_2–95% air. The medium was replaced twice a week. Experiments were performed with cultures that had been maintained for 7 d.

Immunocytochemistry Twenty-four hours before the preparation of cell cultures, the rat pups were injected intraperitoneally with 5-bromo-2′-deoxyuridine (BrdU, 100 mg/kg body weight, in saline; Wako). Seven days after the dissociation, cells were fixed with 4% paraformaldehyde in 0.1 M phosphate buffer (pH 7.4) for 30 min at 4 °C. For DNA denaturation, cells were incubated in 2 M HCl for 30 min at room temperature, rinsed twice with PBS, and incubated in 0.1 M Tris–HCl (pH 7.5) for 5 min. After two washes with PBS, cells were incubated for 1 h in PBS containing 2% normal HS and then incubated overnight at 4 °C in primary antibody (mouse anti-BrdU; Roche, Mannheim, Germany) diluted in the HS-containing PBS. After washing three times with PBS, cells were incubated in secondary antibody (biotinylated horse anti-mouse; Vector Laboratories, Burlingame, CA, U.S.A.) diluted in the HS-containing PBS for 1.5 h and then rinsed three times with PBS. Endogenous peroxidase activity was blocked by incubating the cells in 0.3% H_2O_2 dissolved in methanol for 1 h. After washing three times with PBS, cells were incubated in avidin–biotin–peroxidase complex (ABC Elite kit; Vector Laboratories) for 1 h and then rinsed a further three times with PBS. The BrdU labeling was visualized using 3,3′-diaminobenzidine tetrahydrochloride (DAB; Wako). Cells were preincubated for 5 min in DAB dissolved in PBS (0.2 mg/ml) without H_2O_2, followed by addition of H_2O_2 solution (final concentration, 0.01%). The peroxidase reaction was allowed to proceed for about 5—10 min. Cells were washed repeatedly in PBS, and then rinsed with water. To count BrdU-labeled cells, at least three areas (each $211\times317\ \mu m^2$) were selected randomly for each sample.

Electrophysiology Whole-cell recordings were made with the aid of glass patch pipettes (2—5 MΩ) filled with 100 mM CsCl, 2 mM $MgCl_2$, 10 mM EGTA, 10 mM *N*-(2-hydroxyethyl) piperazine-*N*′-ethanesulfonic acid (Hepes), 15 mM tetraethylammonium chloride, 5 mM Mg-ATP, 20 mM creatine phosphate, and 50 U/ml creatine kinase (the pH was adjusted to 7.3 with CsOH). The external solution contained the following: 130 mM NaCl, 5 mM $CaCl_2$, 2 mM $MgCl_2$, 10 mM Hepes, 10 mM glucose, 5 mM 4-aminopyridine and 500 nM tetrodotoxin (the pH was adjusted to 7.4 with NaOH). Membrane currents were recorded under voltage-clamp conditions using a patch-clamp amplifier (Nihon Kohden, Tokyo, Japan) and data acquisition/analysis software (pCLAMP; Axon Instruments CA, U.S.A.), with filtering at 1 kHz. All of the experiments were performed at room temperature.

Drugs and Their Application The pharmacological properties of the Ca^{2+} current in dentate granule cells were studied by adding the appropriate drugs to the external solution. Nifedipine (Sigma) was prepared as a 500× stock solution in ethanol. Ni^{2+} and Cd^{2+} were freshly prepared daily. In some recordings, Ba^{2+} was used as a charge carrier instead of Ca^{2+}. 4HN (Cayman Chemical, Ann arbor, MI, U.S.A.) was prepared as a 1000× stock solution in ethanol. ω-Conotoxin-GVIA and ω-agatoxin-IVA were purchased from Peptides Institute (Osaka, Japan) and prepared as 100 μM stock solutions in saline. The effects of 4HN on the Ca^{2+} current were studied using 4HN added to Locke's buffer (154 mM NaCl, 5.6 mM KCl, 2.3 mM $CaCl_2$, 1.0 mM $MgCl_2$, 3.6 mM $NaHCO_3$, 10 mM glucose, and 5 mM Hepes, pH 7.2), according to the method described by Mark *et al.*[9] Immediately before experimental treatment, the culture medium was replaced with Locke's buffer. In all experiments, an equivalent volume of vehicle was added to control cultures.

RESULTS

Identification of Dentate Granule Cells The vast majority of neurons in the dentate gyrus of the hippocampus are granule cells,[22] but contamination by a small number of pyramidal cells or interneurons is still possible. To exclude this possibility, we carefully identified dentate granule cells in a prepared cell population based on their size and morphology. Phase-contrast photographs of dentate gyrus cell cultures are shown in Fig. 1A. In these cultures, we observed quite a large number of dentate granule cells, which have small and round or oval cell bodies (Fig. 1A, middle). These cells possessed one or two thin processes. In the same cultures, a subpopulation of neurons different from dentate granule cells was identified. This subpopulation included neurons displaying a pyramidal-cell-like shape (Fig. 1A, right) or a nongranule-cell-, nonpyramidal-cell-like shape (data not shown). To compare granule cells with the remaining neurons, the width and the length of their cell bodies were measured, and the results are summarized as histograms (Fig. 1B.) In our cell cultures, neither the width nor the length of the cell bodies of the total cell population exhibited a Gaussian distribution (Fig. 1B, top). However, the population of dentate granule cells, selected by the visual criteria stated above, exhibited a Gaussian distribution (Fig. 1B, mid-

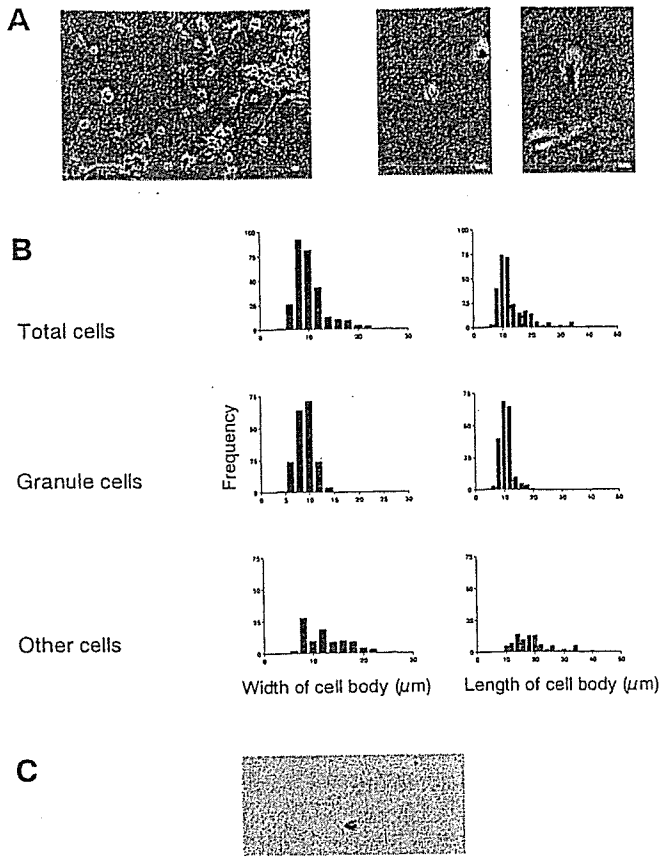

Fig. 1. Neurons in Dentate Gyrus Cultures

A. Phase-contrast photographs of 7-d-cultured dentate gurus cells. Representative photomicrographs showing cultured dentate gyrus neurons (left), a granule cell (middle), and pyramidal cells (right). B. Histograms showing the size distributions of dentate gyrus neurons (the total population of neurons in dentate gyrus cultures is shown at the top, the granule cells are shown in the middle, and the remaining neurons are shown at the bottom). The width (left) and the length of the cell bodies (right) are shown for each cell population. C. Immunochemical identification of newborn dentate granule cells. BrdU-labeled cells are evident in the photomicrograph of dentate gyrus cultures. No BrdU-positive label was observed in neurons other than the granule cells in these cultures (data not shown). The scale bar=10 μm.

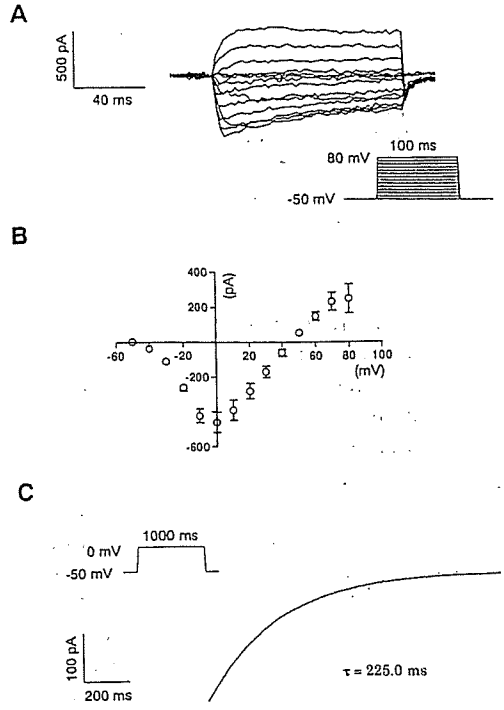

Fig. 2. Ca^{2+} Current in 7-d-Cultured Cells

Outward currents were blocked by Cs^+, tetraethylammonium and 4-aminopyridine. Recordings were made with 500 nM tetrodotoxin to block voltage-gated Na^+ channels. A. Depolarizing command pulses from a holding potential of −50 mV elicited the Ca^{2+} current. B. Averaged current–voltage (*I–V*) relationship of the Ca^{2+} current (n=26). The threshold of activation was at about −30 mV, and the current peaked at 0 mV. Each symbol and bar represent the mean and S.E.M., respectively. C. An example of a single exponential fit to the current decay. The fit was superimposed on an original current trace that was obtained by a command potential to 0 mV.

dle). For these granule cells, the averaged cell body width and length were 8.6±0.1 μm and 10.4±0.2 μm, respectively (mean±S.E.M., n=198). The width and the length of the cell bodies of the remaining "non-granule cells" were 13.5±0.5 μm and 19.4±0.7 μm, respectively (n=110).

Although most mammalian neurons are formed before birth, the production of dentate granule cells continues until adulthood. To examine whether the dentate granule cells identified by our criteria exhibited neurogenesis, we quantified newly generated neurons using BrdU immunochemistry method. As shown in Fig. 1C, we observed BrdU-labeled dentate granule cells, indicating that newly generated dentate granule cells existed in the cultures. From the quantitative analysis, 14.1±2.7% (mean±S.E.M.) of total dentate granule cells were BrdU positive. These results suggest that the dentate granule cells in our cell cultures possessed characteristics similar to those identified *in vivo* with respect to their shape, size, and capacity for neurogenesis, and that dentate granule cells can therefore be distinguished using our criteria.

Whole-cell Ca^{2+} Currents in Dentate Granule Cells Electrophysiological experiments were performed on the cultured dentate granule cells. In many peripheral and central neurons, Ca^{2+} currents can be grouped according to their activation thresholds into low-voltage-activated (LVA) or high-voltage-activated (HVA) Ca^{2+} currents. The LVA currents are activated at between −70 and −40 mV and inactivate rapidly. The HVA currents are activated at around −30 mV and inactivate slowly.[23] Ca^{2+} currents elicited in cultured dentate granule cells by depolarizing voltage steps between −50 and 80 mV are shown in Fig. 2A. The voltage steps were applied for 100 ms from a holding potential of −50 mV. Ca^{2+} currents were activated at −30 mV and more positive potentials, and the maximal current was observed at 0 mV (−459.3±58.1 pA; mean±S.E.M., n=26; Fig. 2B). The current activated by a 1-s depolarizing voltage step exhibited a clear decay, and this decay was analyzed by fitting monoexponential functions (Fig. 2C). The time constant for the decay at 0 mV was 223.0±27.3 ms (n=10).

The HVA currents are characterized by a much higher permeability for Ba^{2+} than for Ca^{2+}.[24] Substitution of Ca^{2+} by an equimolar concentration of Ba^{2+} increases the amplitude of the HVA currents. In the cultured dentate granule cells, the current amplitude was increased by 56.0±13.1% (n=6) at a test pulse of 0 mV when 5 mM Ca^{2+} was replaced by 5 mM Ba^{2+} (Fig. 3A). Inorganic ions such as Ni^{2+} or Cd^{2+} are potent blockers of various types of Ca^{2+} currents. While such divalent ions cause a relatively nonspecific block at concentrations in the millimolar range,[25,26] they show some specificity when used in the micromolar concentration range. In most neurons, 30 μM Cd^{2+} blocks selectively the HVA currents, while the LVA currents remain almost unaffected. In

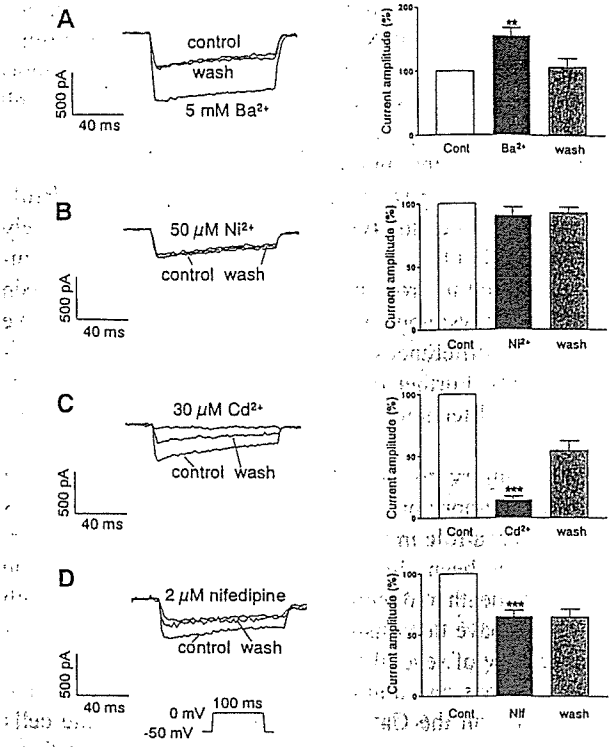

Fig. 3. Effects of Replacement of Ca^{2+} by Ba^{2+} (A) and Application of Ca^{2+} Channel Blockers (B—D) on the Ca^{2+} Current

The Ca^{2+} current was elicited by a voltage step to 0 mV. Representative current traces of Ca^{2+} current (left) and a summary of the averaged data (right) are shown. Also shown are the effects of replacement of 5 mM Ca^{2+} by 5 mM Ba^{2+} (A), 50 μM Ni^{2+} (B), 30 μM Cd^{2+} (C), and 2 μM nifedipine (D). Values are the mean±S.E.M. of data from 5—8 neurons from at least three separate cultures (**$p<0.01$, ***$p<0.001$, paired t-test).

contrast, 50 μM Ni^{2+} preferentially reduces the LVA currents. Figure 3B shows the effect of 50 μM Ni^{2+} on the Ca^{2+} current elicited by a test pulse to 0 mV. The Ca^{2+} current was reduced by 9.4±6.9% on average ($n=6$). With 30 μM Cd^{2+}, the Ca^{2+} current was decreased by 87.8±3.4% ($n=5$; Fig. 3C). Nifedipine, a dihydropyridine HVA Ca^{2+}-current blocker, depressed the Ca^{2+} current by 33.8±6.2% ($n=8$; Fig. 3D).

Effects of 4HN on Ca^{2+} Currents in the Dentate Granule Cells Pretreatment of dentate granule cells with 1 μM 4HN for 2 h resulted in a significant increase (58.1±14.4%) in the amplitude of the Ca^{2+} current. The current amplitude was increased by 28% in neurons exposed to 10 μM 4HN (Fig. 4). The current–voltage relationships in the absence or presence of 4HN showed that the voltage dependence remained unchanged in neurons exposed to 4HN (Fig. 4B). Cultured hippocampal neurons express VGCCs of the L, N, and P/Q types, and the majority of the whole-cell Ca^{2+} current is attributed to L-type Ca^{2+} channels.[27,28] To determine which types of VGCCs were affected by 4HN, we employed pharmacological agents that block specific channel types. In control cultures, addition of 3 μM ω-conotoxin-GVIA, a blocker of N-type Ca^{2+} channels, 2 μM nifedipine, a blocker of L-type Ca^{2+} channels, and 0.3 μM ω-agatoxin-IVA , a blocker of P/Q-type Ca^{2+} channels, resulted in 20.7, 34.8, and 23.0% decreases in the amplitude of the Ca^{2+} current, respectively (Fig. 5B). In 4HN-treated neurons, ω-conotoxin-GVIA caused a 16.4% decrease, nifedipine caused a 90.0% decrease, and ω-agatoxin-IVA caused a 22.8% decrease in the amplitude of the Ca^{2+} current (Fig. 5B). These

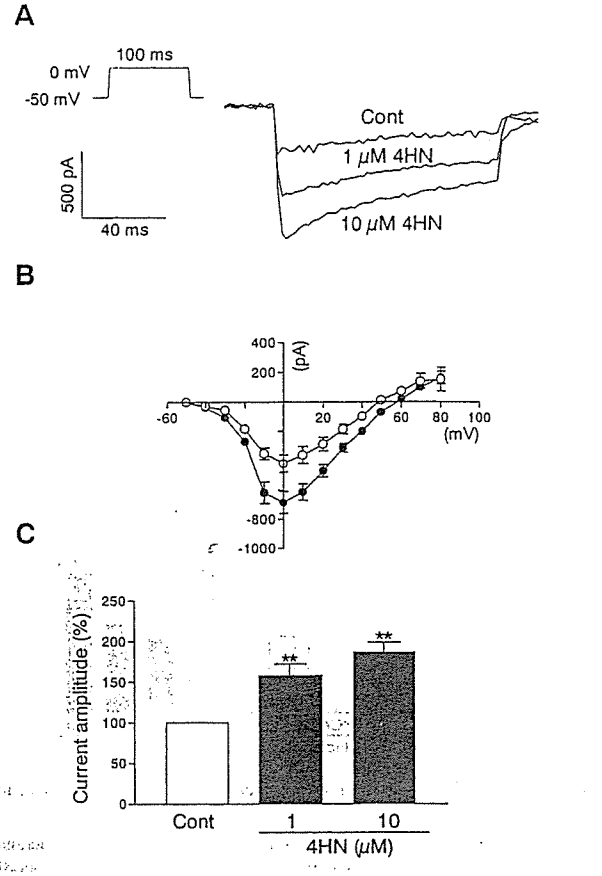

Fig. 4. 4-Hydroxynonenal (4HN) Enhances the Ca^{2+} Current in Dentate Granule Cells

A. Representative recordings of the Ca^{2+} current in cells that had been treated for 2 h with either 1 or 10 μM 4HN. Control cells had been treated with 0.02% ethanol (vehicle). B. Averaged I–V relationship in cells that had been exposed for 2 h to either the vehicle (○, $n=10$) or 10 μM 4HN (●, $n=9$). C. Summarized data of the peak Ca^{2+} current in cells exposed for 2 h to the indicated concentrations of 4HN. Values are the mean±S.E.M. from 10—21 neurons from at least five separate cultures (**$p<0.01$, ANOVA followed by Dunnett's multiple range test).

results suggest that the increase is due mainly to an increase in a current that is mediated through L-type Ca^{2+} channels.

DISCUSSION

In the present study, a dissociated culture system rich in dentate granule cells obtained from postnatal rats was employed to characterize their electrophysiological properties. Although effective electrophysiological studies using adult hippocampal slices have been reported recently, we employed a cell culture system using dissected dentate gyrus and identified dentate granule cells, which we have used previously to examine the effects of 4HN on cell death in various neuronal preparations such as cultured hippocampal neurons,[20] PC12,[19] and cultured cerebellar granule neurons;[18] we have also used this protocol for a preliminarily study of cultured Ammon's horn neurons and dentate gyrus neurons (our unpublished data). Similar culture approaches using dentate gyrus cell have already been reported,[29,30] and the dentate granule cell culture system has been already shown to be a faithful and useful model of mossy fiber sprouting.[6] However, there have not been sufficient analyses of cell properties to allow the identification of dentate granule cells in these studies. In the present study, we carefully identified dentate

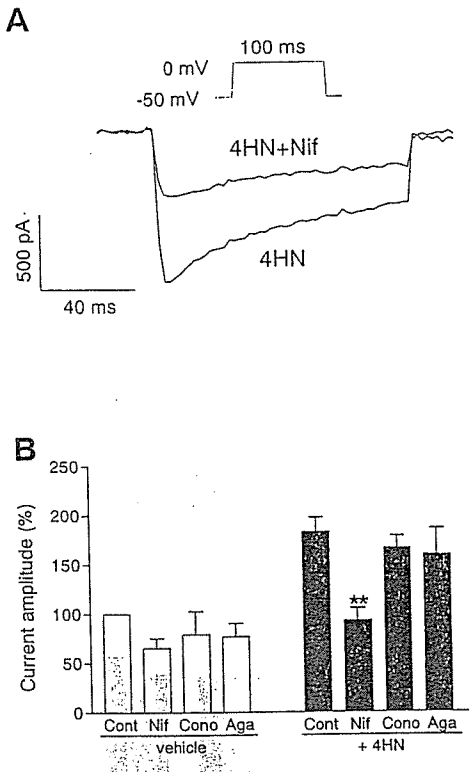

Fig. 5. Effects of Ca^{2+} Channel Blockers on the Ca^{2+} Current in Dentate Granule Cells

A. Representative current traces of the Ca^{2+} current. B. Summarized data of current amplitudes obtained in the absence (Cont) or presence of the blockers for specific subtypes of VGCCs (nifedipine, Nif; ω-conotoxin-GVIA, Cono; ω-agatoxin-IVA, Aga) from control cultures (vehicle; open columns) and cultures treated for 2 h with 10 μM 4HN (+4HN). Values are the mean±S.E.M. from 6—14 neurons. $^{**}p<0.01$ compared with corresponding control values determined by ANOVA followed by Dunnett's multiple range test.

granule cells, and then used these cells for the subsequent investigations. The cells used for the electrophysiological investigations were small in size and round or oval in shape. Their morphological characteristics are consistent with those that have been reported for dentate granule cells.[29] Moreover, the cells were stained with BrdU, a marker of dividing cells, indicating that they possessed the capacity for neurogenesis after birth. These results suggest that the identified cells were indeed dentate granule cells. Therefore, the dentate granule cells identified by our criteria were chosen for experiments including electrophysiological analyses.

High levels of subunit expression of L-type Ca^{2+} channels have been found in the dentate granule cell layer.[7] In the present study, we investigated the basic properties of the Ca^{2+} current using dentate granule cells. The threshold of activation of the Ca^{2+} current in these cells was about −30 mV. The Ca^{2+} current became maximal at 0 mV. Their kinetics compare well with those of the HVA Ca^{2+} currents reported in various other neuronal preparations.[31] With a depolarizing step of 1 s duration, the current decay could be fitted by monoexponential functions. By using the inorganic Ca^{2+} antagonists Cd^{2+}, a HVA Ca^{2+}-current blocker, and Ni^{2+}, a T-type Ca^{2+}-channel blocker, as pharmacological tools, the Ca^{2+} currents in dentate granule cells were characterized further. The Ca^{2+} current in these cells was highly sensitive to a low concentration (30 μM) of Cd^{2+}, as has been reported previously for HVA Ca^{2+} currents.[24,32,33] Unlike the LVA Ca^{2+} currents described previously,[25,26] the Ca^{2+} current in the granule cells was not particularly sensitive to a micromolar concentration (50 μM) of Ni^{2+}. Moreover, nifedipine, a dihydropyridine Ca^{2+}-channel antagonist, blocked a large proportion of the current. These findings are consistent with a high expression of the L-type Ca^{2+} channel shown by *in situ* hybridization and by immunocytochemical studies.[7,34] In the present study, two types of dentate granule cells [*i.e.* BrdU positive (newly generated type) and BrdU negative (relatively mature type) cells] have been found. Although technical limitations prevented us from being able to distinguish between them in electrophysiological experiments, we did not observe any significant differences throughout the electrophysiological experiments. Further detailed investigations using different experimental techniques will be necessary to clarify this problem.

Oxidative injury to neurons in regions responsible for learning and memory processes, such as the hippocampus, is believed to play a role in the pathogenesis of AD.[8,10] Furthermore, 4HN has been shown to play important roles in the neuronal cell death induced by oxidative insults. Although recent reports have demonstrated that oxidative stress modulates the activity of several types of channels in cultured hippocampal neurons and adult rat hippocampal slices,[35,36] the effects of 4HN on the Ca^{2+} current in dentate granule cells are unclear. In the present study, the amplitude of the Ca^{2+} current in 4HN-treated dentate granule cells was significantly larger than in the untreated cells. When L-type Ca^{2+} channels were blocked by nifedipine, the current augmentation by 4HN was canceled, whereas the blocking of N- or P/Q-type channels by ω-conotoxin-GVIA or ω-agatoxin-IVA, respectively, had no effect. It has been reported that the blocking of L-type Ca^{2+} channels attenuates amyloid β protein (Aβ)-induced cell death,[37,38] whereas the blocking of N- or P/Q-type Ca^{2+} channels have little effect.[39] In addition, this Aβ-induced influx of Ca^{2+} is mediated by free radicals. These findings also suggest that oxidative stress increases the Ca^{2+} influx mediated through L-type Ca^{2+} channels.

In the present study, 1—10 μM 4HN significantly enhanced the Ca^{2+} current. These concentrations of 4HN are compatible with those that have been measured in hippocampal neurons after exposure to Aβ.[9] The exact mechanisms whereby 4HN selectively enhances the nifedipine-sensitive Ca^{2+} current in cultured dentate granule cells remain to be elucidated. Currents that originate through VGCCs are known to be increased by the phosphorylation of channel α subunit proteins. Tyrphostins, a family of protein tyrosine kinase inhibitors, protect the nerve cell line HT-22, as well as rat primary neurons, from the cell death induced by oxidative toxicity.[14] In addition, the levels of phosphorylation of the NMDA receptor subunit NR1 are increased in neurons exposed to 4HN.[40] 4HN may directly or indirectly increase phosphorylation of the α subunit of L-type Ca^{2+} channels. L-type Ca^{2+} channels are abundant in dentate granule cells, and so the augmentation of these channels by 4HN may be implicated in pathophysiological processes.

Acknowledgements This work was partly supported by Health and Labour Science Research Grants for Research on Advanced Medical Technology from the Ministry of Health, Labour and Welfare, Japan and a Grant-in-aid for Scientific Research from The Ministry of Education, Culture, Sports,

Science, and Technology, Japan (KAKENHI 13672319) awarded to K.N.

REFERENCES

1) Conrad C. D., Roy E. J., *J. Neurosci.*, **13**, 2582—2590 (1993).
2) Lemaire V., Koehl M., Le Moal M., Abrous D. N., *Proc. Natl. Acad. Sci. U.S.A.*, **97**, 11032—11037 (2000).
3) McNaughton B. L., Barnes C. A., Meltzer J., Sutherland R. J., *Exp. Brain Res.*, **76**, 485—496 (1989).
4) Liu J., Solway K., Messing R. O., Sharp F. R., *J. Neurosci.*, **18**, 7768—7778 (1998).
5) van Praag H., Schinder A. F., Christie B. R., Toni N., Palmer T. D., Gage F. H., *Nature* (London), **415**, 1030—1034 (2002).
6) Ikegaya Y., Nishiyama N., Matsuki N., *Neuroscience*, **98**, 647—659 (2000).
7) Chin H., Smith M. A., Kim H. L., Kim H., *FEBS Lett.*, **299**, 69—74 (1992).
8) Mark R. J., Blanc E. M., Mattson M. P., *Mol. Neurobiol.*, **12**, 211—224 (1996).
9) Mark R. J., Lovell M. A., Markesbery W. R., Uchida K., Mattson M. P., *J. Neurochem.*, **68**, 255—264 (1997).
10) Yankner B. A., *Neuron*, **16**, 921—932 (1996).
11) Urabe T., Yamasaki Y., Hattori N., Yoshikawa M., Uchida K., Mizuno Y., *Neuroscience*, **100**, 241—250 (2000).
12) Ishige K., Schubert D., Sagara Y., *Free Radic. Biol. Med.*, **30**, 433—446 (2001).
13) Ishige K., Chen Q., Sagara Y., Schubert D., *J. Neurosci.*, **21**, 6069—6076 (2001).
14) Sagara Y., Ishige K., Tsai C., Maher P., *J. Biol. Chem.*, **277**, 36204—36215 (2002).
15) Miranda S., Opazo C., Larrondo L. F., Muñoz F. J., Ruiz F., Leighton F., Inestrosa N. C., *Prog. Neurobiol.*, **62**, 633—648 (2000).
16) Yoritaka A., Hattori N., Uchida K., Tanaka M., Stadtman E. R., Mizuno Y., *Proc. Natl. Acad. Sci. U.S.A.*, **93**, 2696—2701 (1996).
17) Pedersen W. A., Fu W., Keller J. N., Markesbery W. R., Appel S., Smith R. G., Kasarskis E., Mattson M. P., *Ann. Neurol.*, **44**, 819—824 (1998).
18) Ito Y., Arakawa M., Ishige K., Fukuda H., *Neurosci. Res.*, **35**, 321—327 (1999).
19) Ito Y., Kosuge Y., Sakikubo T., Horie K., Ishikawa N., Obokata N., Yokoyama E., Yamashina K., Yamamoto M., Saito H., Arakawa M., Ishige K., *Neurosci. Res.*, **46**, 119—125 (2003).
20) Kosuge Y., Koen Y., Ishige K., Minami K., Urasawa H., Saito H., Ito Y., *Neuroscience*, **122**, 885—895 (2003).
21) Rudge J. S., Alderson R. F., Pasnikowski E., McClain J., Ip N.Y., Lindsay R. M., *Eur. J. Neurosci.*, **4**, 459—471 (1992).
22) Seress L., Pokorny J., *J. Anat.*, **133**, 181—195 (1981).
23) Carbone E., Lux H. D., *Nature* (London), **310**, 501—502 (1984).
24) Fox A. P., Nowycky M. C., Tsien R. W., *J. Physiol.*, **394**, 149—172 (1987).
25) Muller T. H., Misgeld U., Swandulla D., *J. Physiol.*, **450**, 341—362 (1992).
26) Ozawa S., Tsuzuki K., Iino M., Ogura A., Kudo Y., *Brain Res.*, **495**, 329—336 (1989).
27) Blalock E. M., Porter N. M., Landfield P. W., *J. Neurosci.*, **19**, 8674—8684 (1999).
28) Furukawa K., Mattson M. P., *J. Neurochem.*, **70**, 1876—1886 (1998).
29) Baranes D., Lopez-Garcia J. C., Chen M., Bailey C. H., Kandel E. R. *Proc. Natl. Acad. Sci. U.S.A.*, **93**, 4706—4711 (1996).
30) Boss B. D., Gozes I., Cowan W. M., *Brain Res.*, **433**, 199—218 (1987).
31) Bean B. P., *Annu. Rev. Physiol.*, **51**, 367—384 (1989).
32) Mogul D. J., Fox A. P., *J. Physiol.*, **433**, 259—281 (1991).
33) Toselli M., Taglietti V., *Neurosci. Lett.*, **112**, 70—75 (1990).
34) Ahlijanian M. K., Westenbroek R. E., Catterall W. A., *Neuron*, **4**, 819—832 (1990).
35) Muller W., Bittner K., *J. Neurophysiol.*, **87**, 2990—2995 (2002).
36) Sah R., Galeffi F., Ahrens R., Jordan G., Schwartz-Bloom R. D., *J. Neurochem.*, **80**, 383—391 (2002).
37) Weiss J. H., Pike C. J., Cotman C. W., *J. Neurochem.*, **62**, 372—375 (1994).
38) Abe K., Kimura H., *J. Neurochem.*, **67**, 2074—2078 (1996).
39) Ueda K., Shinohara S., Yagami T., Asakura K., Kawasaki K., *J. Neurochem.*, **68**, 265—271 (1997).
40) Lu C., Chan S. L., Haughey N., Lee W. T., Mattson M. P., *J. Neurochem.*, **78**, 577—589 (2001).